ON A VORTICITY-BASED FORMULATION FOR REACTION-DIFFUSION-BRINKMAN SYSTEMS

VERÓNICA ANAYA

GIMNAP, Departamento de Matemática
Universidad del Bío-Bío, Concepción, Chile

MOSTAFA BENDAHMANE

Institut de Mathématiques de Bordeaux
Université de Bordeaux, 33076 Bordeaux Cedex, France

DAVID MORA

GIMNAP, Departamento de Matemática
Universidad del Bío-Bío, Concepción, Chile
and
Centro de Investigación en Ingeniería Matemática (CI^{2}MA)
Universidad de Concepción, Concepción, Chile

RICARDO RUIZ BAIER[*]

Mathematical Institute, University of Oxford
A. Wiles Building, Woodstock Road, Oxford OX2 6GG, UK

(Communicated by Christian Rohde)

ABSTRACT. We are interested in modelling the interaction of bacteria and certain nutrient concentration within a porous medium admitting viscous flow. The governing equations in primal-mixed form consist of an advection-reaction-diffusion system representing the bacteria-chemical mass exchange, coupled to the Brinkman problem written in terms of fluid vorticity, velocity and pressure, and describing the flow patterns driven by an external source depending on the local distribution of the chemical species. *A priori* stability bounds are derived for the uncoupled problems, and the solvability of the full system is analysed using a fixed-point approach. We introduce a primal-mixed finite element method to numerically solve the model equations, employing a primal scheme with piecewise linear approximation of the reaction-diffusion unknowns, while the discrete flow problem uses a mixed approach based on Raviart-Thomas elements for velocity, Nédélec elements for vorticity, and piecewise constant pressure approximations. In particular, this choice produces exactly divergence-free velocity approximations. We establish existence of discrete solutions and show their convergence to the weak solution of the continuous coupled problem. Finally, we report several numerical experiments illustrating the behaviour of the proposed scheme.

[*] Corresponding author.

1. **Introduction.** Reaction-diffusion systems can explain many phenomena taking place in diverse disciplines such as industrial and environmental processes, biomedical applications, or population dynamics. For instance, non-equilibrium effects associated to mass exchange and local configuration modifications in the concentration of species are usually represented in terms of classical reaction-diffusion equations. These models allow to reproduce chaos, spatiotemporal patterns, rhythmic and oscillatory scenarios, and many other mechanisms. Nevertheless, in most of these applications the reactions do not occur in complete isolation. The species are rather immersed in a fluid, or they move within (and interact with) a fluid-solid continuum, and the motion of the fluid inevitably affects that of the species. In some circumstances, reciprocal effects might be substantially large, therefore leading to local changes in the observed flow patterns. More specifically, here it is assumed that the medium where the chemical reactions develop is a porous material saturated with an incompressible fluid. We remark that we are interested in viscous flows and consequently, the linear momentum and mass conservation for the fluid are governed by the Brinkman equations. The regime under study is relevant to fluids within highly porous structures composed by light fixed particles [7]. As indicated above, we also suppose that the local fluctuations of a species' concentration is important enough to affect the fluid flow. In turn, the reaction-diffusion equations include additional terms accounting for the advection of each species with the fluid velocity, therefore improving the mixing and interaction properties with respect to those observed under pure diffusion effects [13]. Diverse types of continuum-based models resulting in reaction-diffusion-momentum equations have been applied for e.g. enzyme reactions advected with a known Poiseuille velocity profile [16], population kinetics on moving domains [28, 35], the control of drug release within soft living tissue [9, 15], or biochemical interactions on growing surfaces [12].

We aim at developing numerical solutions to a class of similar systems, also addressing the solvability of the governing equations, the expected properties of the underlying solutions, and the convergence behaviour of suitable finite element schemes. More precisely, at both continuous and discrete levels, the Brinkman equations are set in a mixed form (that is, the associated formulation possesses a saddle-point structure involving the vorticity as additional unknown) whereas the formulation of the reaction-diffusion system is written exclusively in terms of the primal variables, in this case the species' concentration. Such a structure is motivated by the need of accurate vorticity rendering, obtained directly without postprocessing it from typically low-order discrete velocities (which usually leads to insufficiently reliable approximations). The nonlinear reaction-diffusion system will be placed in the framework of general semilinear parabolic equations and its well-posedness, for a fixed velocity, follows from the classical theory of Ladyženskaja [22]. On the other hand, for a fixed species' concentration, a number of recent Brinkman formulations based on vorticity, pressure and velocity are available from the literature [3, 5, 6, 19] (see also [14]). Here we adopt the one introduced in [4], where the well-posedness of the flow equations is established thanks to the classical Babuška-Brezzi framework. In turn, the fully coupled problem is analysed using a Schauder fixed-point approach. Perhaps the closest contributions in the spirit of the present study are the error estimation for finite element formulations to doubly-diffusive Boussinesq flows presented in [2], the two-sidedly degenerate chemotaxis-fluid coupled system from [11] whose solvability relies on a regularisation step combined with

compactness arguments; and the general analysis for degenerate parabolic equations idealising reactive solute transport in porous media recently carried out in [21].

A further goal is to propose a numerical method based on piecewise linear and continuous polynomials for the species' concentrations, whereas the set of flow equations is discretised using a mixed approach based on Raviart-Thomas elements for the approximation of the velocity, Nédélec elements for vorticity, and piecewise constants for the pressure. The computational burden of this algorithm is comparable to classical low-cost approximations as the so-called MINI element for velocity-pressure formulations. On top of that, the proposed finite element method provides divergence-free velocities, thus preserving an essential constraint of the underlying physical system. Based on the present formulation, the stability properties of different staggered coupling techniques have been recently analysed in [24]. Other recent contributions regarding the numerical discretisation for related models for reactive solute transport in porous media (but using Darcy descriptions of flow), include the formulation and convergence studies for mixed and conformal methods as presented in [1, 8, 20, 27, 30, 31].

After this introductory section, the remainder of the paper is structured in the following manner. Section 2 states the model problem and introduces the concept of weak solutions, together with an auxiliary coupled problem. The solvability of these auxiliary equations is established in Section 3, using a fixed-point approach. The proof of uniqueness of weak solution is postponed to Section 4. Section 5 deals with the numerical approximation of the model problem, using mixed finite elements and a first-order backward Euler time advancing scheme. We provide in Section 6 a set of numerical tests to illustrate the properties of the numerical scheme and the features of the coupled model, and we close in Section 7 with a summary and discussion of possible extensions to this work.

2. Governing equations.

2.1. **Problem statement.** Let $\Omega \subset \mathbb{R}^3$, be a simply connected, and bounded porous domain saturated with a Newtonian incompressible fluid, where also a bacterium and some chemical species (diffusible agents or nutrients) are present. Viscous flow in the porous medium is usually modelled with Brinkman equations stating momentum and mass conservation of the fluid. In addition, the Reynolds transport principle applied to mass conservation of the interacting species yields an advection-reaction-diffusion system. The physical scenario of interest can be therefore described by a coupled system written in terms of the fluid velocity $\boldsymbol{u}$, the rescaled fluid vorticity $\boldsymbol{\omega}$, the fluid pressure p, and the volumetric fraction (or concentration) of the bacterium c and of the chemical substance s. Let t denote the time variable taking values in the interval $(0, T]$, where T is a given final time. Then for a.e. $(\boldsymbol{x}, t) \in \Omega_T := \Omega \times (0, T]$, we consider

$$\partial_t c + \boldsymbol{u} \cdot \nabla c - \operatorname{div}(D_c(c)\nabla c) = G_c(c, s), \quad \partial_t s + \boldsymbol{u} \cdot \nabla s - \operatorname{div}(D_s(s)\nabla s) = G_s(c, s),$$

$$\mathbb{K}^{-1}\boldsymbol{u} + \sqrt{\mu}\operatorname{\mathbf{curl}}\boldsymbol{\omega} + \nabla p = s\boldsymbol{g} + \boldsymbol{f}, \quad \boldsymbol{\omega} - \sqrt{\mu}\operatorname{\mathbf{curl}}\boldsymbol{u} = \mathbf{0}, \quad \operatorname{div}\boldsymbol{u} = 0,$$

$$(2.1)$$

where μ is the fluid viscosity (in the considered regime, it is assumed independent of the bacteria and chemical concentrations), $\mathbb{K}(\boldsymbol{x})$ is the permeability tensor rescaled with viscosity, $s\boldsymbol{g}$ represents the force exerted by the bacteria on the fluid motion (where $\boldsymbol{g}$ is the gravitational acceleration, or any other particular force to which the species comply), and $\boldsymbol{f}(\boldsymbol{x}, t)$ is an external force (e.g. centrifugal) applied to

the porous medium. Moreover, D_c, D_s, G_c, G_s are concentration-dependent coefficients determining, respectively, the nonlinear diffusivities and reaction kinetics (representing production and degradation) of bacteria and chemical species.

Equations (2.1) are complemented with the following boundary and initial data:

$$
\begin{aligned}
(c\boldsymbol{u} - D_c(c)\nabla c) \cdot \boldsymbol{n} = (s\boldsymbol{u} - D_s(s)\nabla s) \cdot \boldsymbol{n} = 0 \quad &(\boldsymbol{x}, t) \in \partial\Omega \times (0, T], \\
\boldsymbol{u} \cdot \boldsymbol{n} = u_\partial, \ \boldsymbol{\omega} \times \boldsymbol{n} = \boldsymbol{\omega}_\partial \quad &(\boldsymbol{x}, t) \in \partial\Omega \times (0, T], \\
c = c_0, \ s = s_0 \quad &(\boldsymbol{x}, t) \in \Omega \times \{0\},
\end{aligned}
\tag{2.2}
$$

representing that the species cannot leave the medium and that a normal velocity u_∂ together with a compatible vorticity trace $\boldsymbol{\omega}_\partial$ are imposed along the domain boundary $\partial\Omega$. The presentation will be restricted however to homogeneous boundary conditions. The analysis readily extends to the non-homogeneous case by classical lifting arguments.

2.2. **Main assumptions.** We suppose that the permeability tensor $\mathbb{K} \in [C(\bar{\Omega})]^{3\times 3}$ is symmetric and uniformly positive definite. So is its inverse, i.e., there exists $C > 0$ such that

$$
\boldsymbol{v}^{\mathsf{t}}\mathbb{K}^{-1}(\boldsymbol{x})\boldsymbol{v} \geq C|\boldsymbol{v}|^2 \quad \forall \, \boldsymbol{v} \in \mathbb{R}^3, \ \forall \, \boldsymbol{x} \in \Omega.
\tag{2.3}
$$

In addition, the diffusivities are assumed always positive, coercive, and continuous: for $i \in \{s, c\}$,

$$
D_i : [0, 1] \mapsto \mathbb{R}^+ \text{ is continuous}, \quad 0 < D^{\min} \leq D_i(m) \leq D^{\max} < \infty, \quad m \in \mathbb{R}.
\tag{2.4}
$$

Regarding the reaction terms G_c, G_s, we assume they are continuous functions and there exist constants $C_c, C_s, C > 0$ such that

$$
\begin{aligned}
&|G_c(c, s)| \leq C_c(1 + |c| + |s|), \quad |G_s(c, s)| \leq C_s(1 + |c| + |s|) \text{ for all } c, s \geq 0, \\
&|G_\kappa(c_1, s_1) - G_\kappa(c_2, s_2)| \leq C(|c_1 - c_2| + |s_1 - s_2|), \\
&\qquad\qquad\qquad\qquad\qquad \text{for all } c_1, c_2, s_1, s_2 \geq 0 \text{ and } \kappa = c, s, \\
&G_c(c, s) = \nu_1 \text{ and } G_s(c, s) = \nu_2 \text{ if } c \leq 0 \text{ or } s \leq 0,
\end{aligned}
\tag{2.5}
$$

for some parameters $\nu_1, \nu_2 > 0$. Initial data are assumed nonnegative and regular enough

$$
c_0, s_0 \geq 0, \quad c_0, s_0 \in \mathrm{L}^\infty(\Omega).
\tag{2.6}
$$

Observe that for constant coefficients D_c, D_s, G_c, G_s, problem (2.1) might also serve as a model for the coupling of Newtonian flows with mass and heat transport [32].

2.3. **Weak solutions.** According to (2.2), let us introduce the functional spaces

$$
\begin{aligned}
\mathbf{H}_0(\mathrm{div}; \Omega) &= \left\{ \boldsymbol{v} \in \mathbf{H}(\mathrm{div}; \Omega) : \boldsymbol{v} \cdot \boldsymbol{n} = 0 \text{ on } \partial\Omega \right\}, \\
\mathbf{H}_0(\mathbf{curl}; \Omega) &= \left\{ \boldsymbol{z} \in \mathbf{H}(\mathbf{curl}; \Omega) : \boldsymbol{z} \times \boldsymbol{n} = \mathbf{0} \text{ on } \partial\Omega \right\},
\end{aligned}
$$

where $\mathbf{H}(\mathrm{div}; \Omega)$ is the space of square integrable vectorial functions whose divergence is a scalar square integrable function in Ω. We then proceed, for a given $t > 0$, to test the first two equations in (2.1) with functions in $\mathrm{H}_0^1(\Omega)$, the third equation in (2.1) against functions in $\mathbf{H}_0(\mathrm{div}; \Omega)$, the fourth equation in (2.1) against functions in $\mathbf{H}_0(\mathbf{curl}; \Omega)$ and to integrate by parts. The last equation is tested with functions in $\mathrm{L}^2(\Omega)$ (denoting the scalar space of square integrable functions having zero mean value in Ω) and no integration by parts is applied. Consequently, and using (2.2) we can give the following definition.

Definition 2.1. In view of the properties outlined in Section 2.2, we shall say that the function $(c, s, \boldsymbol{u}, \boldsymbol{\omega}, p)$ is a weak solution to (2.1) if

$$s, c \in \mathrm{L}^\infty(0, T; L^2(\Omega)) \cap \mathrm{L}^2(0, T; \mathrm{H}^1(\Omega)), \quad \partial_t s, \partial_t c \in \mathrm{L}^2(0, T; \mathrm{H}^1(\Omega)'),$$

$$\boldsymbol{u} \in \mathbf{L}^2(0, T; \mathbf{H}(\mathrm{div}; \Omega)), \quad \boldsymbol{\omega} \in \mathbf{L}^2(0, T; \mathbf{H}(\mathbf{curl}; \Omega)), \quad p \in \mathrm{L}^2(0, T; \mathrm{L}^2_0(\Omega)),$$

and

$$\int_0^T \langle \partial_t c, m^c \rangle \, \mathrm{d}t + \iint_{\Omega_T} (D_c(c)\nabla c - c\boldsymbol{u}) \cdot \nabla m^c \, \mathrm{d}\boldsymbol{x}\mathrm{d}t$$

$$= \iint_{\Omega_T} G_c(c, s) m^c \, \mathrm{d}\boldsymbol{x}\mathrm{d}t,$$

$$\int_0^T \langle \partial_t s, m^s \rangle \, \mathrm{d}t + \iint_{\Omega_T} (D_s(s)\nabla s - s\boldsymbol{u}) \cdot \nabla m^s \, \mathrm{d}\boldsymbol{x}\mathrm{d}t$$

$$= \iint_{\Omega_T} G_s(c, s) m^s \, \mathrm{d}\boldsymbol{x}\mathrm{d}t,$$

$$\iint_{\Omega_T} \mathbb{K}^{-1}\boldsymbol{u} \cdot \boldsymbol{v} \, \mathrm{d}\boldsymbol{x}\mathrm{d}t + \sqrt{\mu} \iint_{\Omega_T} \mathbf{curl}\, \boldsymbol{\omega} \cdot \boldsymbol{v} \, \mathrm{d}\boldsymbol{x}\mathrm{d}t - \iint_{\Omega_T} p \, \mathrm{div}\, \boldsymbol{v} \, \mathrm{d}\boldsymbol{x}\mathrm{d}t$$

$$= \iint_{\Omega_T} (s\boldsymbol{g} + \boldsymbol{f}) \cdot \boldsymbol{v} \, \mathrm{d}\boldsymbol{x}\mathrm{d}t,$$

$$\sqrt{\mu} \iint_{\Omega_T} \mathbf{curl}\, \boldsymbol{z} \cdot \boldsymbol{u} \, \mathrm{d}\boldsymbol{x}\mathrm{d}t - \iint_{\Omega_T} \boldsymbol{\omega} \cdot \boldsymbol{z} \, \mathrm{d}\boldsymbol{x}\mathrm{d}t = 0,$$

$$- \iint_{\Omega_T} q \, \mathrm{div}\, \boldsymbol{u} \, \mathrm{d}\boldsymbol{x}\mathrm{d}t = 0,$$

for all $m^i \in \mathrm{L}^2(0, T; \mathrm{H}^1(\Omega))$, $\boldsymbol{v} \in \mathbf{L}^2(0, T; \mathbf{H}_0(\mathrm{div}; \Omega))$, $\boldsymbol{z} \in \mathbf{L}^2(0, T; \mathbf{H}_0(\mathbf{curl}; \Omega))$, $q \in \mathrm{L}^2(0, T; \mathrm{L}^2_0(\Omega))$.

Our first main result states existence of weak solutions to the reaction-diffusion-Brinkman equations. The analysis of uniqueness will be postponed to Section 4.

Theorem 2.2. *Assume that conditions (2.3), (2.4) and (2.5) hold. If $c_0, s_0 \in \mathrm{L}^\infty(\Omega)$ with $c_0 \geq 0$ and $s_0 \geq 0$ a.e. in Ω, then there exists a weak solution of (2.1)-(2.2) in the sense of Definition 2.1. Moreover, the solution (c, s) is nonnegative and bounded in $\mathrm{L}^\infty(\Omega_T, \mathbb{R}^2)$.*

The proof of this result is based on an application of Schauder's fixed-point theorem (in an appropriate functional setting) with the derivation of *a priori* estimates and the compactness arguments, to the following uncoupled system

$$\partial_t c + \boldsymbol{u} \cdot \nabla c - \mathrm{div}(D_c(c)\nabla c) = G_c(c, s), \quad \partial_t s + \boldsymbol{u} \cdot \nabla s - \mathrm{div}(D_s(s)\nabla s) = G_s(c, s),$$

$$\mathbb{K}^{-1}\boldsymbol{u} + \sqrt{\mu}\,\mathbf{curl}\,\boldsymbol{\omega} + \nabla p = \hat{s}\boldsymbol{g} + \boldsymbol{f}, \quad \boldsymbol{\omega} - \sqrt{\mu}\,\mathbf{curl}\,\boldsymbol{u} = \mathbf{0}, \quad \mathrm{div}\,\boldsymbol{u} = 0,$$

$$(2.7)$$

where $\hat{s}$ is a fixed function.

3. **Existence result: Fixed-point approach.** In this section we prove the existence of solutions to (2.7), looking first at the solvability of the uncoupled systems.

3.1. **Preliminaries.** Let us recall the following abstract result (see e.g. [17, Theorem 1.3]):

Theorem 3.1. *Let $(\mathcal{X}, \langle \cdot, \cdot \rangle_{\mathcal{X}})$ be a Hilbert space. Let $\mathcal{A} : \mathcal{X} \times \mathcal{X} \to \mathbb{R}$ be a bounded symmetric bilinear form, and let $\mathcal{G} : \mathcal{X} \to \mathbb{R}$ be a bounded functional. Assume that there exists $\bar{\beta} > 0$ such that*

$$\sup_{\substack{y \in \mathcal{X} \\ y \neq 0}} \frac{\mathcal{A}(x,y)}{\|y\|_{\mathcal{X}}} \geq \bar{\beta} \, \|x\|_{\mathcal{X}} \quad \forall \, x \in \mathcal{X}.$$

Then, there exists a unique $x \in \mathcal{X}$, such that

$$\mathcal{A}(x,y) = \mathcal{G}(y) \quad \forall \, y \in \mathcal{X}.$$

Moreover, there exists $C > 0$, independent of the solution, such that

$$\|x\|_{\mathcal{X}} \leq C \|\mathcal{G}\|_{\mathcal{X}'}.$$

Let us also consider the kernel of the bilinear form $\int_{\Omega} q \operatorname{div} \boldsymbol{u} \, d\boldsymbol{x}$, that is

$$\begin{aligned}
\mathrm{X} := \{ \boldsymbol{v} \in \mathbf{H}_0(\operatorname{div}; \Omega) : & \int_{\Omega} q \operatorname{div} \boldsymbol{v} \, d\boldsymbol{x} = 0, \, \forall q \in \mathrm{L}_0^2(\Omega) \} \\
& = \{ \boldsymbol{v} \in \mathbf{H}_0(\operatorname{div}; \Omega) : \operatorname{div} \boldsymbol{v} = 0 \text{ a.e. in } \Omega \}.
\end{aligned}$$

Moreover, we endow the space $\mathbf{H}(\mathbf{curl}; \Omega)$ with the following μ-dependent norm:

$$\|\boldsymbol{z}\|_{\mathbf{H}(\mathbf{curl};\Omega)}^2 := \|\boldsymbol{z}\|_{0,\Omega}^2 + \mu \| \mathbf{curl} \, \boldsymbol{z}\|_{0,\Omega}^2,$$

and recall the following inf-sup condition (*cf.* [17]): there exists $\beta_2 > 0$ only depending on Ω, such that

$$\sup_{\substack{\boldsymbol{v} \in \mathbf{H}(\operatorname{div};\Omega) \\ \boldsymbol{v} \neq 0}} \frac{\left| \displaystyle\int_{\Omega} q \operatorname{div} \boldsymbol{v} \, d\boldsymbol{x} \right|}{\|\boldsymbol{v}\|_{\mathbf{H}(\operatorname{div};\Omega)}} \geq \beta_2 \|q\|_{0,\Omega} \quad \forall q \in \mathrm{L}_0^2(\Omega). \tag{3.1}$$

3.2. **The fixed-point method.** In view of invoking Schauder's fixed-point theorem to establish solvability of (2.7), we introduce the following closed subset of the Banach space $\mathrm{L}^2(\Omega_T)$:

$$\mathcal{K}_\phi = \{ \phi \in \mathrm{L}^2(\Omega_T) \, : \, 0 \leq \phi(\boldsymbol{x}, t) \leq e^{(\beta - \lambda)t} k_m, \text{ for a.e. } (\boldsymbol{x}, t) \in \Omega_T \}, \tag{3.2}$$

for $\phi \in \{c, s\}$, where $k_m \geq \sup\{\|c_0\|_{\mathrm{L}^\infty(\Omega)}, \|s_0\|_{\mathrm{L}^\infty(\Omega)}\}$, and λ, β are defined in (3.6) and Lemma 3.4, respectively. Our idea is quite simple, for a given $\hat{s} \in \mathcal{K}_s$ we find first the velocity $\boldsymbol{u}$ and then the pair (c, s) solutions of (2.7). Next, and thanks to Theorem 3.1, we can assert the solvability of the Brinkman equations for a fixed $\hat{s} \in \mathcal{K}_s$ and for any $t > 0$.

Lemma 3.2. *Assume that $\hat{s} \in \mathcal{K}_s$. Then, the variational problem*

$$\begin{aligned}
\int_{\Omega} \mathbb{K}^{-1} \boldsymbol{u} \cdot \boldsymbol{v} \, d\boldsymbol{x} + \sqrt{\mu} \int_{\Omega} \mathbf{curl} \, \boldsymbol{\omega} \cdot \boldsymbol{v} \, d\boldsymbol{x} - \int_{\Omega} p \operatorname{div} \boldsymbol{v} \, d\boldsymbol{x} &= \int_{\Omega} (\hat{s} \boldsymbol{g} + \boldsymbol{f}) \cdot \boldsymbol{v} \, d\boldsymbol{x}, \\
\sqrt{\mu} \int_{\Omega} \mathbf{curl} \, \boldsymbol{z} \cdot \boldsymbol{u} \, d\boldsymbol{x} - \int_{\Omega} \boldsymbol{\omega} \cdot \boldsymbol{z} \, d\boldsymbol{x} &= 0, \\
- \int_{\Omega} q \operatorname{div} \boldsymbol{u} \, d\boldsymbol{x} &= 0,
\end{aligned} \tag{3.3}$$

admits a unique solution $(\boldsymbol{u}, \boldsymbol{\omega}, p) \in \mathbf{H}(\mathrm{div}; \Omega) \times \mathbf{H}(\mathbf{curl}; \Omega) \times \mathrm{L}_0^2(\Omega)$. *Moreover, there exists $C > 0$ independent of μ such that*

$$
\begin{aligned}
\|\boldsymbol{u}\|_{\mathbf{H}(\mathrm{div};\Omega)} &+ \|\boldsymbol{\omega}\|_{\mathbf{H}(\mathbf{curl};\Omega)} + \|p\|_{0,\Omega} \\
&\leq C\big(\|\hat{s}\|_{0,\Omega}\|\boldsymbol{g}\|_{\infty,\Omega} + \|\boldsymbol{f}\|_{0,\Omega} + \|u_\partial\|_{-1/2,\partial\Omega} + \|\boldsymbol{\omega}_\partial\|_{-1/2,\partial\Omega}\big).
\end{aligned}
\tag{3.4}
$$

Proof. First, we observe that, owing to the inf-sup condition (3.1), problem (3.3) is equivalent to: Find $(\boldsymbol{u}, \boldsymbol{\omega}) \in \mathrm{X} \times \mathbf{H}(\mathbf{curl}; \Omega)$ such that

$$
\int_\Omega \mathbb{K}^{-1} \boldsymbol{u} \cdot \boldsymbol{v} \, \mathrm{d}\boldsymbol{x} + \sqrt{\mu} \int_\Omega \mathbf{curl}\, \boldsymbol{\omega} \cdot \boldsymbol{v} \, \mathrm{d}\boldsymbol{x} = \int_\Omega (\hat{s}\boldsymbol{g} + \boldsymbol{f}) \cdot \boldsymbol{v} \, \mathrm{d}\boldsymbol{x}, \qquad \forall \boldsymbol{v} \in \mathrm{X},
$$

$$
\sqrt{\mu} \int_\Omega \mathbf{curl}\, \boldsymbol{z} \cdot \boldsymbol{u} \, \mathrm{d}\boldsymbol{x} - \int_\Omega \boldsymbol{\omega} \cdot \boldsymbol{z} \, \mathrm{d}\boldsymbol{x} = 0, \qquad \forall \boldsymbol{z} \in \mathbf{H}_0(\mathbf{curl}; \Omega).
$$

Then, the desired result follows from Theorem 3.1, repeating the argument employed in the proofs of [4, Theorem 2.2 and Corollary 2.1]. $\qquad\square$

On the other hand, given a fixed velocity $\boldsymbol{u} \in \mathbf{L}^2(0, T; \mathbf{H}(\mathrm{div}; \Omega))$, the following result establishes the solvability of the reaction-diffusion system:

Lemma 3.3. *For any $\boldsymbol{u} \in \mathbf{L}^2(0, T; \mathbf{H}(\mathrm{div}; \Omega))$, the system*

$$
\int_0^T \langle \partial_t c, m^c \rangle \, \mathrm{d}t + \iint_{\Omega_T} (D_c(c)\nabla c - c\boldsymbol{u}) \cdot \nabla m^c \, \mathrm{d}\boldsymbol{x}\mathrm{d}t = \iint_{\Omega_T} G_c(c, s)m^c \, \mathrm{d}\boldsymbol{x}\mathrm{d}t,
$$

$$
\int_0^T \langle \partial_t s, m^s \rangle \, \mathrm{d}t + \iint_{\Omega_T} (D_s(s)\nabla s - s\boldsymbol{u}) \cdot \nabla m^s \, \mathrm{d}\boldsymbol{x}\mathrm{d}t = \iint_{\Omega_T} G_s(c, s)m^s \, \mathrm{d}\boldsymbol{x}\mathrm{d}t,
\tag{3.5}
$$

is uniquely solvable and there exists $C > 0$, depending on $\|c_0\|_{0,\Omega}$ and $\|s_0\|_{0,\Omega}$, such that

$$
\|c\|_{\mathrm{L}^2(0,T;\mathrm{H}^1(\Omega))} + \|s\|_{\mathrm{L}^2(0,T;\mathrm{H}^1(\Omega))} \leq C.
$$

Proof. It suffices to combine assumptions (2.4), (2.6) with the general result for quasilinear parabolic problems given in [22, Section 5]. $\qquad\square$

As the next step, we consider a constant $\lambda > 0$ and define the auxiliary variables (ϕ_c, ϕ_s) by setting

$$
c = e^{\lambda t}\phi_c \quad \text{and} \quad s = e^{\lambda t}\phi_s. \tag{3.6}
$$

Then (c, s) satisfies the strong form of (3.5) with diffusion and reaction terms replaced, respectively, by

$$
\begin{cases}
D_c(c) := D_c(e^{\lambda t}c) \text{ and } D_s(s) := D_s(e^{\lambda t}s), \\
G_c(c, s) := -\lambda c + e^{-\lambda t}G_c(e^{\lambda t}c, e^{\lambda t}s), \\
G_s(c, s) := -\lambda s + e^{-\lambda t}G_s(e^{\lambda t}c, e^{\lambda t}s).
\end{cases}
$$

We now introduce a map $\mathcal{R} : \mathcal{K}_s \to \mathcal{K}_s$ such that $\mathcal{R}(\hat{s}) = s$, where s solves (3.5). The goal is to prove that such map has a fixed-point. First, let us show that $\mathcal{R}$ is a continuous mapping. Let $(\hat{s}_n)_n$ be a sequence in $\mathcal{K}_s$ and $\hat{s} \in \mathcal{K}_s$ be such that $\hat{s}_n \to \hat{s}$ in $\mathrm{L}^2(\Omega_T)$ as $n \to \infty$. Let us then define $s_n = \mathcal{R}(\hat{s}_n)$, i.e., s_n is the solution of (3.5) associated with $\hat{s}_n$ and the solution $\boldsymbol{u}$ of (3.3). The objective is to show that s_n converges to $\mathcal{R}(\hat{s})$ in $\mathrm{L}^2(\Omega_T)$. We start with the following lemma:

Lemma 3.4. *Let $(c_n, s_n)_n$ be the solution to problem (3.5) and recall that $\hat{s} \in \mathcal{K}_s$. Then*

(i) *There exists a constant $\gamma \geq 0$ such that $0 \leq c_n(\boldsymbol{x}, t), s_n(\boldsymbol{x}, t) \leq e^{\gamma t} k_m$, for a.e.*
    $(\boldsymbol{x}, t) \in \Omega_T$, where k_m is defined as in (3.2).
(ii) *The sequence $(c_n, s_n)_n$ is bounded in $\mathrm{L}^2(0, T; \mathrm{H}^1(\Omega, \mathbb{R}^2)) \cap \mathrm{L}^\infty(0, T; \mathrm{L}^2(\Omega, \mathbb{R}^2))$.*
(iii) *The sequence $(\partial_t c_n, \partial_t s_n)_n$ is bounded in $\mathrm{L}^2(0, T; (\mathrm{H}^1(\Omega, \mathbb{R}^2))')$.*
(iv) *The sequence $(c_n, s_n)_n$ is relatively compact in $\mathrm{L}^2(\Omega_T)$.*

Proof. (*i*) We replace the strong form of (3.5) by

$$\partial_t c_n - \mathrm{div}(D_c(c_n)\nabla c_n) + \boldsymbol{u} \cdot \nabla c_n = -\lambda c_n + e^{-\lambda t} G_c(e^{\lambda t} c_n, e^{\lambda t} s_n), \qquad \text{in } \Omega_T. \quad (3.7)$$

Multiplying (3.7) by $-c_n^- = \dfrac{c_n - |c_n|}{2}$ and integrating over Ω, we obtain

$$\frac{1}{2}\frac{d}{dt}\int_\Omega |c_n^-|^2 d\boldsymbol{x} + D^{\min}\int_\Omega |\nabla c_n^-|^2 d\boldsymbol{x} - \int_\Omega c_n^- \boldsymbol{u} \cdot \nabla c_n d\boldsymbol{x} - \lambda \int_\Omega c_n c_n^- d\boldsymbol{x}$$
$$\leq -\int_\Omega e^{-\lambda t} G_c(e^{\lambda t} c_n, e^{\lambda t} s_n) c_n^- d\boldsymbol{x}. \quad (3.8)$$

Now, we use that $\mathrm{div}\,\boldsymbol{u} = 0$ and (2.5) to deduce

$$-\int_\Omega c_n^- \boldsymbol{u} \cdot \nabla c_n \, d\boldsymbol{x} = \frac{1}{2}\int_\Omega \boldsymbol{u} \cdot \nabla(c_n^-)^2 \, d\boldsymbol{x} = 0,$$

and

$$\begin{cases} -\int_\Omega e^{-\lambda t} G_c(e^{\lambda t} c_n, e^{\lambda t} s_n) c_n^- \, d\boldsymbol{x} \leq 0 & \text{if } c_n \leq 0, \\ -\int_\Omega e^{-\lambda t} G_c(e^{\lambda t} c_n, e^{\lambda t} s_n) c_n^- \, d\boldsymbol{x} = 0 & \text{if } c_n > 0. \end{cases}$$

According to the positivity of the second and the fourth terms in the left-hand side of (3.8), we get

$$\frac{1}{2}\frac{d}{dt}\int_\Omega |c_n^-|^2 \, d\boldsymbol{x} \leq 0.$$

Since c_0 is nonnegative, we deduce that $c_n^- = 0$, and reasoning similarly we have that $s_n^- = 0$.

Next, we let $k_c, k_s \in \mathbb{R}$ such that $k_c \geq \|c_0\|_{\mathrm{L}^\infty(\Omega)}$ and $k_s \geq \|s_0\|_{\mathrm{L}^\infty(\Omega)}$. Let us consider $t \in (0, T)$, and proceed to multiply (3.7) by

$$\xi_c := (c_n - e^{(\beta-\lambda)t} k)^+, \quad \text{with } \beta \geq \lambda, \text{ and with } k = \sup\{k_c, k_s\},$$

and to integrate over Ω, which yields that there exists some constant $C_6 > 0$ such that

$$\frac{1}{2}\frac{d}{dt}\int_\Omega \xi_c^2 \, d\boldsymbol{x} + (\beta - \lambda)\int_\Omega e^{(\beta-\lambda)t} k\,\xi_c \, d\boldsymbol{x} + D^{\min}\int_\Omega |\nabla \xi_c|^2 \, d\boldsymbol{x}$$
$$+ \int_\Omega \xi_c \, \boldsymbol{u} \cdot \nabla c_n \, d\boldsymbol{x} + \lambda \int_\Omega c_n \,\xi_c d\boldsymbol{x}$$
$$= \frac{1}{2}\frac{d}{dt}\int_\Omega \xi_c^2 \, d\boldsymbol{x} + \beta \int_\Omega e^{(\beta-\lambda)t} k\,\xi_c \, d\boldsymbol{x} + D^{\min}\int_\Omega |\nabla \xi_c|^2 \, d\boldsymbol{x}$$
$$+ \frac{1}{2}\int_\Omega \boldsymbol{u} \cdot (\nabla \xi_c^2) \, d\boldsymbol{x} + \lambda \int_\Omega \xi_c^2 \, d\boldsymbol{x}$$
$$\leq \int_\Omega e^{-\lambda t} G_c(e^{\lambda t} c_n, e^{\lambda t} s_n) \xi_c \, d\boldsymbol{x}$$
$$\leq C_6 \left(\int_\Omega e^{(\beta-\lambda)t} k\,\xi_c \, d\boldsymbol{x} + \int_\Omega \xi_c^2 \, d\boldsymbol{x} + \int_\Omega \xi_s^2 \, d\boldsymbol{x} \right), \quad (3.9)$$

where $\xi_s := (s_n - e^{(\beta-\lambda)t}k)^+$. Following an analogous treatment for s_n, we get

$$\frac{1}{2}\frac{d}{dt}\int_\Omega \xi_s^2\,d\boldsymbol{x} + (\beta-\lambda)\int_\Omega e^{(\beta-\lambda)t}k\xi_s\,d\boldsymbol{x} + D^{\min}\int_\Omega |\nabla\xi_s|^2\,d\boldsymbol{x}$$
$$+ \int_\Omega \xi_s \boldsymbol{u}\cdot\nabla s_n\,d\boldsymbol{x} + \lambda\int_\Omega s_n\xi_s\,d\boldsymbol{x}$$
$$\leq C_7\left(\int_\Omega e^{(\beta-\lambda)t}k\xi_s\,d\boldsymbol{x} + \int_\Omega \xi_c^2\,d\boldsymbol{x} + \int_\Omega \xi_s^2\,d\boldsymbol{x}\right), \qquad (3.10)$$

for some constant $C_7 > 0$. We next observe that

$$\int_\Omega \boldsymbol{u}\cdot\nabla(\xi_c)^2\,d\boldsymbol{x} = 0, \quad \int_\Omega \boldsymbol{u}\cdot\nabla(\xi_s)^2\,d\boldsymbol{x} = 0,$$

which inserted into (3.9) and (3.10), implies that

$$\frac{1}{2}\frac{d}{dt}\int_\Omega \xi_c^2\,d\boldsymbol{x}$$
$$+ \frac{1}{2}\frac{d}{dt}\int_\Omega \xi_s^2\,d\boldsymbol{x} + (\beta - C_6 - C_7)e^{(\beta-\lambda)t}k\left(\int_\Omega \xi_c\,d\boldsymbol{x} + \int_\Omega \xi_s\,d\boldsymbol{x}\right) \qquad (3.11)$$
$$+ (\lambda - C_6 - C_7)\int_\Omega \xi_c^2\,d\boldsymbol{x} + (\lambda - C_6 - C_7)\int_\Omega \xi_s^2\,d\boldsymbol{x} \leq 0.$$

Finally for $\beta \geq \lambda \geq C_6 + C_7$, an application of (3.11) yields

$$\frac{d}{dt}\int_\Omega |\xi_c|^2\,d\boldsymbol{x} + \frac{d}{dt}\int_\Omega |\xi_s|^2\,d\boldsymbol{x} \leq 0,$$

and exploiting that $c_0, s_0 \leq k$ in Ω, we conclude that $c_n(\cdot, t) \leq e^{(\beta-\lambda)t}k$ and $s_n(\cdot, t) \leq e^{(\beta-\lambda)t}k$ in $\Omega \times (0, T)$.

(ii) We multiply equation (3.7) by c_n and integrate over Ω to obtain

$$\frac{1}{2}\frac{d}{dt}\int_\Omega |c_n|^2\,d\boldsymbol{x} + D^{\min}\int_\Omega |\nabla c_n|^2\,d\boldsymbol{x} + \int_\Omega c_n\boldsymbol{u}\cdot\nabla c_n\,d\boldsymbol{x} + \lambda\int_\Omega |c_n|^2\,d\boldsymbol{x}$$
$$\leq \int_\Omega e^{-\lambda t}G_c(e^{\lambda t}c_n, e^{\lambda t}s_n)c_n\,d\boldsymbol{x}. \qquad (3.12)$$

Invoking the boundedness of c_n and s_n, we get that the integral on the right-hand side is bounded independently of n. Then using that

$$\int_\Omega c_n\boldsymbol{u}\cdot\nabla c_n\,d\boldsymbol{x} = \frac{1}{2}\int_\Omega \boldsymbol{u}\cdot\nabla(c_n)^2\,d\boldsymbol{x} = 0,$$

we deduce from (3.12) the following bound

$$\frac{1}{2}\frac{d}{dt}\int_\Omega |c_n|^2\,d\boldsymbol{x} + D^{\min}\int_\Omega |\nabla c_n|^2\,d\boldsymbol{x} \leq C_8,$$

valid for some constant $C_8 > 0$ independent of n. This completes the proof of (ii).

(iii) Next, we multiply (3.7) by $\varphi \in \mathrm{L}^2(0, T; \mathrm{H}^1(\Omega))$ and use the boundedness of c_n and s_n to get

$$\left|\int_0^T \langle\partial_t c_n, \varphi\rangle\,dt\right|$$
$$= \left|-\int_\Omega D_c(c_n)\nabla c_n\cdot\varphi\,d\boldsymbol{x} + \int_\Omega c_n\boldsymbol{u}\cdot\nabla\varphi\,d\boldsymbol{x}\right.$$

$$\left. -\lambda \int_\Omega c_n \varphi \, \mathrm{d}\boldsymbol{x} + \int_\Omega e^{-\lambda t} G_c(e^{\lambda t} c_n, e^{\lambda t} s_n) \varphi \, \mathrm{d}\boldsymbol{x} \right|$$

$$\leq D^{\max} \|\nabla c_n\|_{\mathrm{L}^2(\Omega_T)} \|\varphi\|_{\mathrm{L}^2(\Omega_T)} + C_9 \|\boldsymbol{u}\|_{0,\Omega} \|\nabla \varphi\|_{\mathrm{L}^2(\Omega_T)}$$

$$+ C_{10} \Big(\|c_n\|_{\mathrm{L}^2(\Omega_T)} + \|s_n\|_{\mathrm{L}^2(\Omega_T)} \Big) \|\varphi\|_{\mathrm{L}^2(\Omega_T)}$$

$$\leq C_{11} \|\varphi\|_{\mathrm{L}^2(0,T;\mathrm{H}^1(\Omega))},$$

for some constants $C_9, C_{10}, C_{11} > 0$ independent of n. Consequently, we end up with the bound

$$\|\partial_t c_n\|_{\mathrm{L}^2(0,T;(H^1(\Omega))')} \leq C_{11}. \tag{3.13}$$

Working on the same lines as for $(c_n)_n$, the counterpart of $(ii) - (iii)$ and (3.13) for $(s_n)_n$ can be obtained. Finally, (iv) is deduced from (ii) and (iii). □

In summary, Lemmas 3.2, and 3.4 imply that there exists

$$(c, s, \boldsymbol{u}, \boldsymbol{\omega}, p) \in \mathrm{L}^2(0,T;\mathrm{H}^1(\Omega))^2 \times \mathbf{H}(\mathrm{div};\Omega) \times \mathbf{H}(\mathbf{curl};\Omega) \times \mathrm{L}_0^2(\Omega)$$

such that, up to extracting subsequences if necessary,

$$\begin{cases} (c_n, s_n) \to (c, s) \text{ in } \mathrm{L}^2(\Omega_T, \mathbb{R}^2) \text{ strongly and a.e., and in } \mathrm{L}^2(0,T;\mathrm{H}^1(\Omega)) \text{ weakly}, \\ (\boldsymbol{u}_n, \boldsymbol{\omega}_n, p_n) \to (\boldsymbol{u}, \boldsymbol{\omega}, p) \text{ in } \mathbf{H}(\mathrm{div};\Omega) \times \mathbf{H}(\mathbf{curl};\Omega) \times \mathrm{L}_0^2(\Omega) \text{ weakly}, \end{cases}$$

and consequently, the continuity of $\mathcal{R}$ on $\mathcal{K}_s$ holds. Moreover, Lemma 3.4 indicates the boundedness of $\mathcal{R}(\mathcal{K}_s)$ within the set

$$\mathcal{S} = \left\{ s \in \mathrm{L}^2(0,T;\mathrm{H}^1(\Omega)) \ : \ \partial_t s \in \mathrm{L}^2(0,T;(\mathrm{H}^1(\Omega))') \right\}. \tag{3.14}$$

Appealing to the theory of compact sets [33], the compactness of the map $\mathcal{S} \hookrightarrow \mathrm{L}^2(\Omega_T)$ implies that of $\mathcal{R}$. Therefore, and thanks to Schauder's fixed-point theorem, the operator $\mathcal{R}$ has a fixed point s. That is, there exists a solution to

$$\int_0^T \langle \partial_t c, m^c \rangle \, \mathrm{d}t + \iint_{\Omega_T} (D_c(c)\nabla c - c\boldsymbol{u}) \cdot \nabla m^c \, \mathrm{d}\boldsymbol{x}\mathrm{d}t = \iint_{\Omega_T} G_c(c,s) m^c \, \mathrm{d}\boldsymbol{x}\mathrm{d}t,$$

$$\int_0^T \langle \partial_t s, m^s \rangle \, \mathrm{d}t + \iint_{\Omega_T} (D_s(s)\nabla s - s\boldsymbol{u}) \cdot \nabla m^s \, \mathrm{d}\boldsymbol{x}\mathrm{d}t = \iint_{\Omega_T} G_s(c,s) m^s \, \mathrm{d}\boldsymbol{x}\mathrm{d}t,$$

$$\iint_{\Omega_T} \mathbb{K}^{-1}\boldsymbol{u} \cdot \boldsymbol{v} \, \mathrm{d}\boldsymbol{x}\mathrm{d}t + \sqrt{\mu} \iint_{\Omega_T} \boldsymbol{v} \cdot \mathbf{curl}\,\boldsymbol{\omega} \, \mathrm{d}\boldsymbol{x}\mathrm{d}t - \iint_{\Omega_T} p \, \mathrm{div}\,\boldsymbol{v} \, \mathrm{d}\boldsymbol{x}\mathrm{d}t \tag{3.15}$$

$$\iint_{\Omega_T} (s\boldsymbol{g} + \boldsymbol{f}) \cdot \boldsymbol{v} \, \mathrm{d}\boldsymbol{x}\mathrm{d}t,$$

$$\sqrt{\mu} \iint_{\Omega_T} \boldsymbol{u} \cdot \mathbf{curl}\,\boldsymbol{z} \, \mathrm{d}\boldsymbol{x}\mathrm{d}t - \iint_{\Omega_T} \boldsymbol{\omega} \cdot \boldsymbol{z} \, \mathrm{d}\boldsymbol{x}\mathrm{d}t = 0,$$

$$- \iint_{\Omega_T} q \, \mathrm{div}\,\boldsymbol{u} \, \mathrm{d}\boldsymbol{x}\mathrm{d}t = 0,$$

for all $m^i \in \mathrm{L}^2(0,T;\mathrm{H}^1(\Omega))$, $\boldsymbol{v} \in \mathbf{L}^2(0,T;\mathbf{H}_0(\mathrm{div};\Omega))$, $\boldsymbol{z} \in \mathbf{L}^2(0,T;\mathbf{H}_0(\mathbf{curl};\Omega))$, $q \in \mathrm{L}^2(0,T;\mathrm{L}_0^2(\Omega))$.

4. **Uniqueness of weak solutions.** The following result completes the analysis of unique solvability for the reaction-diffusion-Brinkman system.

Theorem 4.1. *Assume* (2.3)-(2.5) *hold, and let* $(c_1, s_1, \boldsymbol{u}_1, \boldsymbol{\omega}_1, p_1), (c_2, s_2, \boldsymbol{u}_2, \boldsymbol{\omega}_2, p_2)$ *be two weak solutions to* (2.1)-(2.2), *associated with the data* $c_0 = c_{1,0}$, $s_0 = s_{1,0}$,

$\boldsymbol{g} = \boldsymbol{g}_1$, $\boldsymbol{f} = \boldsymbol{f}_1$ *and* $c_0 = c_{2,0}$, $s_0 = s_{2,0}$, $\boldsymbol{g} = \boldsymbol{g}_2$, $\boldsymbol{f} = \boldsymbol{f}_2$, *respectively. Then, for any* $t \in (0, T]$ *there exists* $C > 0$ *such that*

$$\iint_{\Omega_t} \left(|\mathcal{C}|^2 + |\mathcal{S}|^2 + |\mathcal{U}|^2 + |\mathcal{W}|^2 + |\mathcal{P}|^2 \right) \mathrm{d}\boldsymbol{x}\, \mathrm{d}\sigma$$

$$\leq C \Bigg(\int_\Omega \left(|c_{1,0}(\boldsymbol{x}) - c_{2,0}(\boldsymbol{x})|^2 + |s_{1,0}(\boldsymbol{x}) - s_{2,0}(\boldsymbol{x})|^2 \right) \mathrm{d}\boldsymbol{x} \tag{4.1}$$

$$+ \iint_{\Omega_t} \left(|\boldsymbol{g}_1 - \boldsymbol{g}_2|^2 + |\boldsymbol{f}_1 - \boldsymbol{f}_2|^2 \right) \mathrm{d}\boldsymbol{x}\, \mathrm{d}\sigma \Bigg),$$

where $\mathcal{C} = c_1 - c_2$, $\mathcal{S} = s_1 - s_2$, $\mathcal{U} = \boldsymbol{u}_1 - \boldsymbol{u}_2$, $\mathcal{W} = \boldsymbol{\omega}_1 - \boldsymbol{\omega}_2$, *and* $\mathcal{P} = p_1 - p_2$. *In particular, there exists at most one weak solution to the reaction-diffusion-Brinkman system* (2.1)-(2.2).

Proof. First, we observe that the $(\mathcal{U}, \mathcal{W}, \mathcal{P})$ satisfies

$$\iint_{\Omega_t} \mathbb{K}^{-1} \mathcal{U} \cdot \boldsymbol{v}\, \mathrm{d}\boldsymbol{x}\, \mathrm{d}\sigma + \sqrt{\mu} \iint_{\Omega_t} \boldsymbol{v} \cdot \mathbf{curl}\, \mathcal{W}\, \mathrm{d}\boldsymbol{x}\, \mathrm{d}\sigma - \iint_{\Omega_t} \mathcal{P} \operatorname{div} \boldsymbol{v}\, \mathrm{d}\boldsymbol{x}\, \mathrm{d}\sigma$$

$$= \iint_{\Omega_t} (s_1 \boldsymbol{g}_1 - s_2 \boldsymbol{g}_2) \cdot \boldsymbol{v}\, \mathrm{d}\boldsymbol{x}\, \mathrm{d}\sigma + \iint_{\Omega_t} (\boldsymbol{f}_1 - \boldsymbol{f}_2) \cdot \boldsymbol{v}\, \mathrm{d}\boldsymbol{x}\, \mathrm{d}\sigma\,,$$

$$\sqrt{\mu} \iint_{\Omega_t} \mathcal{U} \cdot \mathbf{curl}\, \boldsymbol{z}\, \mathrm{d}\boldsymbol{x}\, \mathrm{d}\sigma - \iint_{\Omega_t} \mathcal{W} \cdot \boldsymbol{z}\, \mathrm{d}\boldsymbol{x}\, \mathrm{d}\sigma = 0,$$

$$- \iint_{\Omega_t} q \operatorname{div} \mathcal{U}\, \mathrm{d}\boldsymbol{x}\, \mathrm{d}\sigma = 0,$$

$$\tag{4.2}$$

for $t \in (0, T)$ and for all $\boldsymbol{v} \in \mathbf{L}^2(0, T; \mathbf{H}_0(\operatorname{div}; \Omega))$, $\boldsymbol{z} \in \mathbf{L}^2(0, T; \mathbf{H}_0(\mathbf{curl}; \Omega))$, $q \in \mathrm{L}^2(0, T; \mathrm{L}_0^2(\Omega))$.

After substituting $\boldsymbol{v} = \mathcal{U}$, $z = \mathcal{W}$, $q = \mathcal{P}$ in (4.2) and adding the resulting equations, we can invoke the continuous dependence on the data (3.4) to establish the *a priori* bound

$$\iint_{\Omega_t} |\mathcal{U}|^2\, \mathrm{d}\boldsymbol{x}\, \mathrm{d}\sigma + \iint_{\Omega_t} |\mathcal{W}|^2\, \mathrm{d}\boldsymbol{x}\, \mathrm{d}\sigma + \iint_{\Omega_t} |\mathcal{P}|^2\, \mathrm{d}\boldsymbol{x}\, \mathrm{d}\sigma$$

$$\leq C_{14} \iint_{\Omega_t} |\mathcal{S}|^2\, \mathrm{d}\boldsymbol{x}\, \mathrm{d}\sigma + C_{15} \left(\iint_{\Omega_t} |\boldsymbol{g}_1 - \boldsymbol{g}_2|^2\, \mathrm{d}\boldsymbol{x}\, \mathrm{d}\sigma + \iint_{\Omega_t} |\boldsymbol{f}_1 - \boldsymbol{f}_2|^2\, \mathrm{d}\boldsymbol{x}\, \mathrm{d}\sigma \right),$$

$$\tag{4.3}$$

for some constant $C_{15} > 0$. Next, note that $(\mathcal{C}, \mathcal{S})$ satisfies

$$- \int_0^t \langle \mathcal{C}, \partial_t m^c \rangle\, \mathrm{d}\sigma + \iint_{\Omega_t} (D_c(c_1) \nabla c_1 - D_c(c_2) \nabla c_2) \cdot \nabla m^c\, \mathrm{d}\boldsymbol{x}\, \mathrm{d}\sigma$$

$$- \iint_{\Omega_t} c_1 \mathcal{U} \cdot \nabla m^c\, \mathrm{d}\boldsymbol{x}\, \mathrm{d}\sigma - \iint_{\Omega_t} \mathcal{C} \boldsymbol{u}_2 \cdot \nabla m^c\, \mathrm{d}\boldsymbol{x}\, \mathrm{d}\sigma$$

$$= \int_\Omega \mathcal{C}_0(\boldsymbol{x}) m^c(\boldsymbol{x}, 0)\, \mathrm{d}\boldsymbol{x} + \iint_{\Omega_t} (G_c(c_1, s_1) - G_c(c_2, s_2)) m^c\, \mathrm{d}\boldsymbol{x}\, \mathrm{d}\sigma\,, \tag{4.4}$$

$$- \int_0^t \langle \mathcal{S}, \partial_t m^s \rangle\, \mathrm{d}\sigma + \iint_{\Omega_t} (D_s(s_1) \nabla s_1 - D_s(s_2) \nabla s_2) \cdot \nabla m^s\, \mathrm{d}\boldsymbol{x}\, \mathrm{d}\sigma$$

$$-\iint_{\Omega_t} s_1 \mathcal{U} \cdot \nabla m^s \, \mathrm{d}\boldsymbol{x} \, \mathrm{d}\sigma - \iint_{\Omega_t} \mathcal{S} \boldsymbol{u}_2 \cdot \nabla m^s \, \mathrm{d}\boldsymbol{x} \, \mathrm{d}\sigma$$

$$= \int_{\Omega} \mathcal{S}_0(\boldsymbol{x}) m^c(\boldsymbol{x}, 0) \, \mathrm{d}\boldsymbol{x} + \iint_{\Omega_t} (G_s(c_1, s_1) - G_s(c_2, s_2)) m^s \, \mathrm{d}\boldsymbol{x} \, \mathrm{d}\sigma \, ,$$

for $t \in (0, T)$ and for all $m^i \in \mathrm{L}^2(0, T; \mathrm{H}^1(\Omega))$ and $\partial_t m^i \in \mathrm{L}^2(0, T; (\mathrm{H}^1(\Omega))')$ with $m^c(\cdot, T) = 0$, $i = c, s$. Now, for $t_0 \in (0, T)$ we take

$$m^i(\boldsymbol{x}, t) = \begin{cases} \displaystyle\int_t^{t_0} (\mathcal{D}_i(i_1) - \mathcal{D}_i(i_2)) \, \mathrm{d}\sigma & \text{for } 0 \le t < t_0, \\ 0 & \text{for } t_0 \le t \le T, \end{cases}$$

where the function $\mathcal{D}$ is the so-called Kirchhoff transform (see for e.g. [25]) $\mathcal{D}_i(i) := \int_0^i D_i(r) \, dr$, for $i = c, s$. Using these relations in (4.4), and recalling that the function $\mathcal{D}$ is strictly increasing, we get

$$-\int_0^T \langle \mathcal{C}, \partial_t m^c \rangle \, \mathrm{d}\sigma = \int_0^{t_0} \langle \mathcal{C}, (\mathcal{D}_c(c_1) - \mathcal{D}_c(c_2)) \rangle \, \mathrm{d}\sigma \ge C_{\mathcal{D}} \iint_{\Omega_{t_0}} |\mathcal{C}|^2 \, \mathrm{d}\boldsymbol{x} \, \mathrm{d}\sigma \, , \quad (4.5)$$

$$\iint_{\Omega_t} (D_c(c_1) \nabla c_1 - D_c(c_2) \nabla c_2) \cdot \nabla m^c \, \mathrm{d}\boldsymbol{x} \, \mathrm{d}\sigma$$

$$= \frac{1}{2} \int_{\Omega} \left| \nabla \int_0^{t_0} (\mathcal{D}_c(c_1) - \mathcal{D}_c(c_2)) \, \mathrm{d}\sigma \right|^2 \, \mathrm{d}\boldsymbol{x},$$

$$\int_{\Omega} \mathcal{C}_0(\boldsymbol{x}) m^c(\boldsymbol{x}, 0) \, \mathrm{d}\boldsymbol{x} = \int_t^{t_0} \int_{\Omega} \mathcal{C}_0(\boldsymbol{x}) (\mathcal{D}_c(c_1) - \mathcal{D}_c(c_2)) \, \mathrm{d}\boldsymbol{x} \, \mathrm{d}\sigma$$

$$\le C_{16} \int_{\Omega} |\mathcal{C}_0(\boldsymbol{x})|^2 \, \mathrm{d}\boldsymbol{x} + \frac{C_{\mathcal{D}}}{4} \iint_{\Omega_{t_0}} |\mathcal{C}|^2 \, \mathrm{d}\boldsymbol{x} \, \mathrm{d}\sigma \, ,$$

for some constants $C_{\mathcal{D}}, C_{16} > 0$. Moreover,

$$\iint_{\Omega_t} c_1 \mathcal{U} \cdot \nabla m^c \, \mathrm{d}\boldsymbol{x} \, \mathrm{d}\sigma \le C_{17} \int_0^{t_0} \iint_{\Omega_t} |\mathcal{U}|^2 \, \mathrm{d}\boldsymbol{x} \, \mathrm{d}\sigma \, \mathrm{d}t$$

$$+ \frac{1}{8} \int_{\Omega} \left| \nabla \int_0^{t_0} (\mathcal{D}_c(c_1) - \mathcal{D}_c(c_2)) \, \mathrm{d}\sigma \right|^2 \, \mathrm{d}\boldsymbol{x},$$

$$\iint_{\Omega_t} \mathcal{C} \boldsymbol{u}_2 \cdot \nabla m^c \, \mathrm{d}\boldsymbol{x} \, \mathrm{d}\sigma \le C_{18} \int_0^{t_0} \iint_{\Omega_t} |\mathcal{C}|^2 \, \mathrm{d}\boldsymbol{x} \, \mathrm{d}\sigma \, \mathrm{d}t$$

$$+ \frac{1}{8} \int_{\Omega} \left| \nabla \int_0^{t_0} (\mathcal{D}_c(c_1) - \mathcal{D}_c(c_2)) \, \mathrm{d}\sigma \right|^2 \, \mathrm{d}\boldsymbol{x},$$

$$(4.6)$$

for some constants $C_{17}, C_{18} > 0$ depending on $\|c_1\|_{\mathrm{L}^\infty(\Omega_T)}$ and $\|\boldsymbol{u}_2\|_{\mathrm{L}^\infty(\Omega_T, \mathbb{R}^3)}$ (the latter being bounded thanks to classical maximal regularity results for Stokes equations cf. [36]). Next, we use (2.5) and the L^∞-bounds of (c_1, s_1) and (c_2, s_2), leading to

$$\iint_{\Omega_t} (G_s(c_1, s_1) - G_s(c_2, s_2)) m^s \, \mathrm{d}\boldsymbol{x} \, \mathrm{d}\sigma \le C_{19} \int_0^{t_0} \left(\iint_{\Omega_t} (|\mathcal{C}|^2 + |\mathcal{S}|^2) \, \mathrm{d}\boldsymbol{x} \, \mathrm{d}\sigma \right) \mathrm{d}t$$

$$+ \frac{C_{\mathcal{D}}}{4} \iint_{\Omega_{t_0}} |\mathcal{C}|^2 \, \mathrm{d}\boldsymbol{x} \, \mathrm{d}\sigma \, ,$$

$$(4.7)$$

for some constant $C_{19} > 0$. We proceed to collect the results (4.3) and (4.5)-(4.7), to infer that

$$\frac{C_{\mathcal{D}}}{2} \iint_{\Omega_{t_0}} |\mathcal{C}|^2 \, \mathrm{d}\boldsymbol{x} \, \mathrm{d}\sigma \leq C_{16} \int_{\Omega} |\mathcal{C}_0(\boldsymbol{x})|^2 \, \mathrm{d}\boldsymbol{x}$$

$$+ C_{20} \left(\iint_{\Omega_t} |\boldsymbol{g}_1 - \boldsymbol{g}_2|^2 \, \mathrm{d}\boldsymbol{x} \, \mathrm{d}\sigma + \iint_{\Omega_t} |\boldsymbol{f}_1 - \boldsymbol{f}_2|^2 \, \mathrm{d}\boldsymbol{x} \, \mathrm{d}\sigma \right)$$

$$+ C_{21} \int_0^{t_0} \left(\iint_{\Omega_t} (|\mathcal{C}|^2 + |\mathcal{S}|^2) \, \mathrm{d}\boldsymbol{x}\mathrm{d}\sigma \right) \mathrm{d}t,$$

(4.8)

for some constants $C_{20}, C_{21} > 0$. Similarly we get for the equation of $\mathcal{S}$

$$\frac{C_{\mathcal{D}}}{2} \iint_{\Omega_{t_0}} |\mathcal{S}|^2 \, \mathrm{d}\boldsymbol{x} \, \mathrm{d}\sigma \leq C_{22} \int_{\Omega} |\mathcal{S}_0(\boldsymbol{x})|^2 \, \mathrm{d}\boldsymbol{x}$$

$$+ C_{23} \left(\iint_{\Omega_t} |\boldsymbol{g}_1 - \boldsymbol{g}_2|^2 \, \mathrm{d}\boldsymbol{x}\mathrm{d}\sigma + \iint_{\Omega_t} |\boldsymbol{f}_1 - \boldsymbol{f}_2|^2 \, \mathrm{d}\boldsymbol{x}\mathrm{d}\sigma \right)$$

$$+ C_{24} \int_0^{t_0} \left(\iint_{\Omega_t} (|\mathcal{C}|^2 + |\mathcal{S}|^2) \, \mathrm{d}\boldsymbol{x}\mathrm{d}\sigma \right) \mathrm{d}t,$$

(4.9)

for some constants $C_{22}, C_{23}, C_{24} > 0$. Thus (4.8) and (4.9) imply

$$\iint_{\Omega_{t_0}} (|\mathcal{C}|^2 + |\mathcal{S}|^2) \, \mathrm{d}\boldsymbol{x} \, \mathrm{d}\sigma \leq C_{25} \int_{\Omega} \left(|\mathcal{C}_0(\boldsymbol{x})|^2 + |\mathcal{S}_0(\boldsymbol{x})|^2 \right) \mathrm{d}\boldsymbol{x}$$

$$+ C_{26} \int_0^{t_0} \left(\iint_{\Omega_t} (|\mathcal{C}|^2 + |\mathcal{S}|^2) \, \mathrm{d}\boldsymbol{x}\mathrm{d}\sigma \right) \mathrm{d}t$$

$$+ C_{27} \left(\iint_{\Omega_t} |\boldsymbol{g}_1 - \boldsymbol{g}_2|^2 \, \mathrm{d}\boldsymbol{x}\mathrm{d}\sigma + \iint_{\Omega_t} |\boldsymbol{f}_1 - \boldsymbol{f}_2|^2 \, \mathrm{d}\boldsymbol{x}\mathrm{d}\sigma \right),$$

(4.10)

for some constants $C_{25}, C_{26}, C_{27} > 0$. Then, an application of Gronwall's inequality to (4.10) combined with (4.3) proves (4.1). $\qquad\square$

5. **Numerical approximation.** In this section, we construct a primal-mixed fully-discrete scheme for the approximation of the coupled system (2.1). The finite element spaces characterising the semi-discrete problem are then specified, and a proof of convergence to the unique weak solution (presented in Definition 2.1) is outlined.

5.1. **The semi-discrete scheme.** Let $\mathcal{T}_h$ be a regular family of triangulations of $\bar{\Omega}$ by tetrahedra K of maximum diameter h. Given an integer $k \geq 0$ and $S \subset \mathbb{R}^3$, by $\mathcal{P}_k(S)$ we denote the space of polynomial functions defined in S of total degree up to k, and define the following finite element subspaces

$$\mathrm{V}_h = \left\{ m_h \in \mathrm{H}^1(\Omega) : m_h|_K \in \mathcal{P}_1(K) \, \forall K \in \mathcal{T}_h \right\},$$

$$\mathbf{H}_h = \left\{ \boldsymbol{v}_h \in \mathbf{H}_0(\mathrm{div}; \Omega) : \boldsymbol{v}_h|_K \in \mathbf{RT}_0(K) \, \forall K \in \mathcal{T}_h \right\},$$

$$\mathbf{Z}_h = \left\{ \boldsymbol{z}_h \in \mathbf{H}(\mathbf{curl}, \Omega) : \boldsymbol{z}_h|_K \in \mathbf{ND}_1(K) \, \forall K \in \mathcal{T}_h \right\},$$

$$\mathrm{Q}_h = \left\{ q_h \in \mathrm{L}_0^2(\Omega) : q_h|_K \in \mathcal{P}_0(K) \, \forall K \in \mathcal{T}_h \right\},$$

(5.1)

where for any $K \in \mathcal{T}_h(\Omega)$, the local lowest order Raviart-Thomas and edge space of Nédélec type, are defined as $\mathbf{RT}_0(K) = \mathcal{P}_0(K)^3 \oplus \mathcal{P}_0(K)\boldsymbol{x}$, and $\mathbf{ND}_1(K) = \mathcal{P}_0(K)^3 \oplus \mathcal{P}_0(K)^3 \times \boldsymbol{x}$, respectively.

Then, a Galerkin semi-discretisation associated to the formulation introduced in Definition 2.1 reads: For $t \in (0, T]$ find $(c_h(t), s_h(t), \boldsymbol{u}_h(t), \boldsymbol{\omega}_h(t), p_h(t)) \in V_h \times V_h \times \mathbf{H}_h \times \mathbf{Z}_h \times Q_h$ such that

$$\int_\Omega \partial_t c_h(t) m_h^c \, \mathrm{d}\boldsymbol{x} + \int_\Omega (D_c(c_h(t)) \nabla c_h(t) - c_h(t)\boldsymbol{u}_h) \cdot \nabla m_h^c \, \mathrm{d}\boldsymbol{x}$$
$$= \int_\Omega G_c(c_h(t), s_h(t)) m_h^c \, \mathrm{d}\boldsymbol{x},$$
$$\int_\Omega \partial_t s_h(t) m_h^s \, \mathrm{d}\boldsymbol{x} + \int_\Omega (D_s(s_h(t)) \nabla s_h(t) - s_h(t)\boldsymbol{u}_h) \cdot \nabla m_h^s \, \mathrm{d}\boldsymbol{x}$$
$$= \int_\Omega G_s(c_h(t), s_h(t)) m_h^s \, \mathrm{d}\boldsymbol{x}, \tag{5.2}$$
$$\int_\Omega \mathbb{K}^{-1}\boldsymbol{u}_h(t) \cdot \boldsymbol{v}_h \, \mathrm{d}\boldsymbol{x} + \sqrt{\mu} \int_\Omega \mathbf{curl}\, \boldsymbol{v}_h \cdot \boldsymbol{\omega}_h(t) \, \mathrm{d}\boldsymbol{x} - \int_\Omega p_h(t) \operatorname{div} \boldsymbol{v}_h \, \mathrm{d}\boldsymbol{x}$$
$$= \int_\Omega (s_h(t)\boldsymbol{g} + \boldsymbol{f}) \cdot \boldsymbol{v}_h \, \mathrm{d}\boldsymbol{x},$$
$$\sqrt{\mu} \int_\Omega \mathbf{curl}\, \boldsymbol{u}_h(t) \cdot \boldsymbol{z}_h \, \mathrm{d}\boldsymbol{x} - \int_\Omega \boldsymbol{\omega}_h(t) \cdot \boldsymbol{z}_h \, \mathrm{d}\boldsymbol{x} = 0,$$
$$-\int_\Omega q_h \operatorname{div} \boldsymbol{u}_h(t) \, \mathrm{d}\boldsymbol{x} = 0,$$

for all $m_h^c, m_h^s \in V_h$, $\boldsymbol{v}_h \in \mathbf{H}_h$, $\boldsymbol{z}_h \in \mathbf{Z}_h$, and $q_h \in Q_h$.

5.2. **Euler time discretisation.** Let $c_h^0 = \mathbb{P}_{V_h}(c_0)$, $s_h^0 = \mathbb{P}_{V_h}(s_0)$ be appropriate projections of the initial data, and consider the following fully discrete method arising after backward Euler time discretisation using a fixed time step $\Delta t = T/N$: For $n \in \{1, \ldots, N\}$, find $(c_h^n, s_h^n, \boldsymbol{u}_h^n, \boldsymbol{\omega}_h^n, p_h^n) \in V_h \times V_h \times \mathbf{H}_h \times \mathbf{Z}_h \times Q_h$ such that

$$\int_\Omega \frac{c_h^n - c_h^{n-1}}{\Delta t} m_h^c \, \mathrm{d}\boldsymbol{x} + \int_\Omega (D_c(c_h^n) \nabla c_h^n - c_h^n \boldsymbol{u}_h^n) \cdot \nabla m_h^c \, \mathrm{d}\boldsymbol{x}$$
$$= \int_\Omega G_c(c_h^{n-1}, s_h^{n-1}) m_h^c \, \mathrm{d}\boldsymbol{x},$$
$$\int_\Omega \frac{s_h^n - s_h^{n-1}}{\Delta t} m_h^c \, \mathrm{d}\boldsymbol{x} + \int_\Omega (D_s(s_h^n) \nabla s_h^n - s_h^n \boldsymbol{u}_h^n) \cdot \nabla m_h^s \, \mathrm{d}\boldsymbol{x}$$
$$= \int_\Omega G_s(c_h^{n-1}, s_h^{n-1}) m_h^s \, \mathrm{d}\boldsymbol{x}, \tag{5.3}$$
$$\int_\Omega \mathbb{K}^{-1}\boldsymbol{u}_h^n \cdot \boldsymbol{v}_h \, \mathrm{d}\boldsymbol{x} + \sqrt{\mu} \int_\Omega \boldsymbol{v}_h \cdot \mathbf{curl}\, \boldsymbol{\omega}_h^n \, \mathrm{d}\boldsymbol{x} - \int_\Omega p_h^n \operatorname{div} \boldsymbol{v}_h \, \mathrm{d}\boldsymbol{x}$$
$$= \int_\Omega (s_h^n \boldsymbol{g} + \boldsymbol{f}) \cdot \boldsymbol{v}_h \, \mathrm{d}\boldsymbol{x},$$
$$\sqrt{\mu} \int_\Omega \boldsymbol{u}_h^n \cdot \mathbf{curl}\, \boldsymbol{z}_h \, \mathrm{d}\boldsymbol{x}\mathrm{d}\mathrm{t} - \int_\Omega \boldsymbol{\omega}_h^n \cdot \boldsymbol{z}_h \, \mathrm{d}\boldsymbol{x} = 0,$$
$$-\int_\Omega q_h \operatorname{div} \boldsymbol{u}_h^n \, \mathrm{d}\boldsymbol{x} = 0,$$

for all $m_h^c, m_h^s \in V_h$, $\boldsymbol{v}_h \in \mathbf{H}_h$, $\boldsymbol{z}_h \in \mathbf{Z}_h$, $q_h \in Q_h$, where the forcing term in the momentum equation is discretised explicitly. We also stress that, owing to the choice (5.1), the discrete velocities $\boldsymbol{u}_h$ generated using either (5.2) or (5.3) are exactly divergence-free, that is, div $\boldsymbol{u}_h(t) = 0$ and div $\boldsymbol{u}_h^n = 0$ in Ω (*cf.* [4]).

5.3. **Sketched convergence analysis.** Note that the positive and negative cuts test functions may not be admissible in finite element context. Therefore, we cannot obtain the maximum principle as in the continuous case. Comparing to the continuous case, here we assume that the initial condition (c_0, s_0) is only in $L^2(\Omega, \mathbb{R}^2)$.

In order to derive stability estimates, we employ the same kind of test functions in the same combination of equations used in Section 3; whereas the chain rule for time derivatives is now replaced by the convexity inequality

$$a^n(a^n - a^{n-1}) \geq \frac{|a^n|^2}{2} - \frac{|a^{n-1}|^2}{2},$$

to treat the finite difference discretisation of the time derivatives. Proceeding in this way, we can obtain estimates (uniform in both h and Δt) for the discrete Brinkman solutions

$$\|\boldsymbol{u}_h\|_{\mathbf{L}^2(0,T;\mathbf{H}(\mathrm{div};\Omega))} + \|\boldsymbol{\omega}_h\|_{\mathbf{L}^2(0,T;\mathbf{H}(\mathbf{curl};\Omega))} + \|p_h\|_{\mathbf{L}^2(0,T;\mathrm{L}_0^2(\Omega))} \leq C, \qquad (5.4)$$

and for the advection-reaction-diffusion system

$$\|c_h\|_{\mathrm{L}^\infty(0,T;\mathrm{L}^2(\Omega))} + \|s_h\|_{\mathrm{L}^\infty(0,T;\mathrm{L}^2(\Omega))} + \|\nabla c_h\|_{\mathrm{L}^2(\Omega_T)} + \|\nabla s_h\|_{\mathrm{L}^2(\Omega_T)} \leq C, \quad (5.5)$$

for some constant $C > 0$.

The next goal is to establish the relative compactness in $\mathrm{L}^2(\Omega_T)$ of the sequences (c_h, s_h), which is achieved by constructing space and time translates and using the *a priori* estimates given above.

Lemma 5.1. *There exists a constant $C > 0$ depending on Ω, T, c_0 and s_0 such that*

$$\iint_{\Omega_{\boldsymbol{r}} \times (0,T)} \left[|c_h(\boldsymbol{x} + \boldsymbol{r}, t) - c_h(\boldsymbol{x}, t)|^2 + |s_h(\boldsymbol{x} + \boldsymbol{r}, t) - s_h(\boldsymbol{x}, t)|^2 \right] \mathrm{d}\boldsymbol{x}\,\mathrm{d}t$$
$$\leq \mathcal{C}\,|\boldsymbol{r}|^2, \qquad (5.6)$$

$$\iint_{\Omega \times (0,T-\tau)} \left[|c_h(\boldsymbol{x}, t + \tau) - c_h(\boldsymbol{x}, t)|^2 + |s_h(\boldsymbol{x}, t + \tau) - s_h(\boldsymbol{x}, t)|^2 \right] \mathrm{d}\boldsymbol{x}\,\mathrm{d}t$$
$$\leq C(\tau + \Delta t). \qquad (5.7)$$

for all $\boldsymbol{r} \in \mathbb{R}^3$ and for all $\tau \in (0, T)$, where $\Omega_{\boldsymbol{r}} = \{\boldsymbol{x} \in \Omega, [\boldsymbol{x}, \boldsymbol{x} + \boldsymbol{r}] \subset \Omega\}$.

Proof. Let us introduce the space translates

$$(J^{\boldsymbol{r}} c_h)(\boldsymbol{x}, \cdot) = c_h(\boldsymbol{x} + \boldsymbol{r}, \cdot) - c_h(\boldsymbol{x}, \cdot), \quad \text{and} \quad (J^{\boldsymbol{r}} s_h)(\boldsymbol{x}, \cdot) = s_h(\boldsymbol{x} + \boldsymbol{r}, \cdot) - s_h(\boldsymbol{x}, \cdot).$$

From the $\mathrm{L}^2(0, T; \mathrm{H}^1(\Omega))$−estimate for c_h and s_h, the bound

$$\int_0^T \int_{\Omega_{\boldsymbol{r}}} |J^{\boldsymbol{r}} c_h|^2 \,\mathrm{d}\boldsymbol{x}\,\mathrm{d}t + \int_0^T \int_{\Omega_{\boldsymbol{r}}} |J^{\boldsymbol{r}} s_h|^2 \,\mathrm{d}\boldsymbol{x}\,\mathrm{d}t \leq \mathcal{C}|\boldsymbol{r}|^2, \qquad (5.8)$$

easily follows. It is then clear that the right-hand side in (5.8) vanishes as $|\boldsymbol{r}| \to 0$, uniformly in h, which yields (5.6).

Next we introduce the time translates

$$(T^h c_h)(\cdot, t) := c_h(\cdot, t + \tau) - c_h(\cdot, t) \text{ and } (T^h s_h)(\cdot, t) := s_h(\cdot, t + \tau) - s_h(\cdot, t),$$

and notice that for all $t \in (0, T - \tau]$, these functions assume values in V_h (cf. (5.1)). Therefore they can be used as test functions in the fully-discrete scheme (5.3). Moreover, the previously proved uniform bounds for (c_h, s_h) and $(\nabla c_h, \nabla s_h)$ in $L^2(\Omega_T, \mathbb{R}^2)$ imply analogous bounds for the translates $T^\tau c_h, T^\tau s_h$ and $\nabla T^\tau c_h$, $\nabla T^\tau s_h$ in $L^2((0, T - \tau) \times \Omega)$.

Let us now define $(\bar{c}_h, \bar{s}_h)$ as the piecewise affine in t function in $W^{1,\infty}((0; T]; V_h)$ interpolating the states $(c_h^n, s_h^n)_{n=0,\ldots,N} \subset V_h$ at the points $(n\Delta t)_{n=0,\ldots,N}$ (recall the interpolation scheme $\bar{n}_h = n_h^{n-1} + \dfrac{t - t_{n-1}}{\Delta t}(n_h^n - n_h^{n-1})$ for $n = c, s$). Then we have

$$
\begin{aligned}
\int_\Omega \partial_t \bar{c}_h \, m_h^c \, \mathrm{d}\boldsymbol{x} + \int_\Omega (D_c(c_h)\nabla c_h - c_h \boldsymbol{u}_h) \cdot \nabla m_h^c \, \mathrm{d}\boldsymbol{x} &= \int_\Omega G_c(c_h, s_h) m_h^c \, \mathrm{d}\boldsymbol{x}, \\
\int_\Omega \partial_t \bar{s}_h \, m_h^s \, \mathrm{d}\boldsymbol{x} + \int_\Omega (D_s(s_h)\nabla s_h - s_h \boldsymbol{u}_h) \cdot \nabla m_h^s \, \mathrm{d}\boldsymbol{x} &= \int_\Omega G_s(c_h, s_h) m_h^s \, \mathrm{d}\boldsymbol{x},
\end{aligned}
\tag{5.9}
$$

for all $m_h^c, m_h^s \in V_h$. We integrate (5.9) with respect to time $\sigma \in [t, t + \tau]$ (with $0 < \tau < T$) and consider $m_h^c = T^\tau c_h$ and $m_h^s = T^\tau s_h$ as test functions in the resulting equations. Therefore

$$
\begin{aligned}
&\int_0^{T-\tau} \int_\Omega \left| (T^h \bar{c}_h)(\boldsymbol{x}, t) \right|^2 \, \mathrm{d}\boldsymbol{x} \, \mathrm{d}t + \int_0^{T-\tau} \int_\Omega \left| (T^h \bar{s}_h)(\boldsymbol{x}, t) \right|^2 \, \mathrm{d}\boldsymbol{x} \, \mathrm{d}t \\
&= \int_0^{T-\tau} \int_\Omega \left(\int_t^{t+\tau} \partial_\sigma \bar{c}_h(\boldsymbol{x}, \sigma) \, \mathrm{d}\sigma \right) (T^h c_h)(\boldsymbol{x}, t) \, \mathrm{d}\boldsymbol{x} \, \mathrm{d}t \\
&\quad + \int_0^{T-\tau} \int_\Omega \left(\int_t^{t+\tau} \partial_\sigma \bar{s}_h(\boldsymbol{x}, \sigma) \, \mathrm{d}\sigma \right) (T^h s_h)(\boldsymbol{x}, t) \, \mathrm{d}\boldsymbol{x} \, \mathrm{d}t \\
&= -\int_0^{T-\tau} \int_\Omega \int_t^{t+\tau} (D_c(c_h)\nabla c_h(\boldsymbol{x}, \sigma) - c_h(\boldsymbol{x}, t)) \boldsymbol{u}_h(\boldsymbol{x})) \cdot \nabla (T^h c_h)(\boldsymbol{x}, t) \, \mathrm{d}\boldsymbol{x} \, \mathrm{d}\sigma \, \mathrm{d}t \\
&\quad - \int_0^{T-\tau} \int_\Omega \int_t^{t+\tau} (D_s(s_h)\nabla s_h(\boldsymbol{x}, \sigma) - s_h(\boldsymbol{x}, t)) \boldsymbol{u}_h(\boldsymbol{x})) \cdot \nabla (T^h s_h)(\boldsymbol{x}, t) \, \mathrm{d}\boldsymbol{x} \, \mathrm{d}\sigma \, \mathrm{d}t \\
&\quad + \int_0^{T-\tau} \int_\Omega \int_t^{t+\tau} G_c(c_h(\boldsymbol{x}, t), s_h(\boldsymbol{x}, t))(T^h c_h)(\boldsymbol{x}, t) \, \mathrm{d}\boldsymbol{x} \, \mathrm{d}\sigma \, \mathrm{d}t \\
&\quad + \int_0^{T-\tau} \int_\Omega \int_t^{t+\tau} G_s(c_h(\boldsymbol{x}, t), s_h(\boldsymbol{x}, t))(T^h s_h)(\boldsymbol{x}, t) \, \mathrm{d}\boldsymbol{x} \, \mathrm{d}\sigma \, \mathrm{d}t \\
&=: I_1 + I_2 + I_3 + I_4.
\end{aligned}
$$

Now, we examine these integrals separately. For I_1 we have

$$
\begin{aligned}
|I_1| \leq C &\left[\int_0^{T-\tau} \int_\Omega \left(\int_t^{t+\tau} |\nabla c_h(\boldsymbol{x}, \sigma)|^2 \, \mathrm{d}\sigma \right)^2 \mathrm{d}\boldsymbol{x} \, \mathrm{d}t \right]^{\frac{1}{2}} \\
&\times \left[\int_0^{T-\tau} \int_\Omega \left| \nabla (T^h c_h)(\boldsymbol{x}, t) \right|^2 \mathrm{d}\boldsymbol{x} \, \mathrm{d}t \right]^{\frac{1}{2}} \leq C \, \tau,
\end{aligned}
$$

and similarly $|I_2| \leq C\,\tau$, for some constant $C > 0$. Herein we have used the Fubini theorem (recall that $\int_t^{t+\tau} \mathrm{d}\sigma = \tau = \int_{\sigma-\tau}^\sigma \mathrm{d}t$), the divergence-free condition for the discrete velocity, the Hölder inequality and the L^2−bounds for (c_h, s_h), $(\nabla c_h, \nabla s_h)$ and $(\nabla T^h c_h, \nabla T^h s_h)$. Keeping in mind the growth assumptions on G_c, G_s, we can then apply Cauchy-Schwarz inequality to deduce that $|I_3| + |I_4| \leq C\,\tau$, for some

constant $C > 0$. Collecting these inequalities we readily get

$$\int_0^{T-\tau} \int_\Omega \left(|\bar{c}_h(\cdot, t+\tau) - \bar{c}_h(\cdot, t)|^2 + |\bar{s}_h(\cdot, t+\tau) - \bar{s}_h(\cdot, t)|^2 \right) d\boldsymbol{x}\, dt \le \mathcal{C}\,\tau.$$

Furthermore, the definition of $(\bar{c}_h, \bar{s}_h)$ together with (5.5) eventually implies that

$$\|\bar{c}_h - c_h\|_{L^2(\Omega_T)}^2 \le \sum_{n=1}^N \Delta t \|c_h^n - c_h^{n-1}\|_{L^2(\Omega)}^2 \le \mathcal{C}(\Delta t) \ \to 0 \ \text{ as } \Delta t \to 0,$$

$$\|\bar{s}_h - s_h\|_{L^2(\Omega_T)}^2 \le \sum_{n=1}^N \Delta t \|s_h^n - s_h^{n-1}\|_{L^2(\Omega)}^2 \le \mathcal{C}(\Delta t) \ \to 0 \ \text{ as } \Delta t \to 0,$$

which establishes (5.7), therefore finishing the proof. $\qquad\square$

Note that as a consequence of (5.4)-(5.5), Lemma 5.1, and Kolmogorov's compactness criterion (*cf.* [10, Theorem IV.25]), we can assert that there exists a subsequence of $(c_h, s_h, \boldsymbol{u}_h, \boldsymbol{\omega}_h, p_h)$, not re-labeled, such that, as $h \to 0$,

$(c_h, s_h) \to (c, s)$ strongly in $L^2(\Omega_T, \mathbb{R}^2)$ and in $L^2(0, T; H^1(\Omega, \mathbb{R}^2))$ weakly,

$(\boldsymbol{u}_h, \boldsymbol{\omega}_h, p_h) \to (\boldsymbol{u}, \boldsymbol{\omega}, p)$

$\qquad$ in $\mathbf{L}^2(0, T; \mathbf{H}(\mathrm{div}; \Omega)) \times \mathbf{L}^2(0, T; \mathbf{H}(\mathbf{curl}; \Omega)) \times L^2(0, T; L_0^2(\Omega))$ weakly.

These convergences allow us to identify the limit $(c, s, \boldsymbol{u}, \boldsymbol{\omega}, p)$ as the weak solution of (2.1), and the convergence result is summarised as follows.

Theorem 5.2. *Assume that conditions* (2.3), (2.4) *and* (2.5) *hold. If* $c_0, s_0 \in L^2(\Omega)$, *then the finite element solution* $(c_h^n, s_h^n, \boldsymbol{u}_h^n, \boldsymbol{\omega}_h^n, p_h^n)$, *generated by* (5.3), *converges along a subsequence to* $(c, s, \boldsymbol{u}, \boldsymbol{\omega}, p)$ *as* $h, \Delta t \to 0$, *where* $(c, s, \boldsymbol{u}, \boldsymbol{\omega}, p)$ *is a weak solution of* (2.1)-(2.2) *in the sense of Definition* 2.1.

We observe that the error generated by the fully discrete scheme (5.3) has two components: one due to the spatial discretisation and depending on the meshsize h, and the error due to the time discretisation depending on the timestep Δt. Given the approximation properties of the employed finite element spaces and the time stepping method (see e.g. [37]), we can expect the following convergence rates for the proposed method

$$\|(c(\cdot, t_n), s(\cdot, t_n), \boldsymbol{u}(\cdot, t_n), \boldsymbol{\omega}(\cdot, t_n), p(\cdot, t_n)) - (c_h^n, s_h^n, \boldsymbol{u}_h^n, \boldsymbol{\omega}_h^n, p_h^n)\| \le C_1 h + C_2 \Delta t,$$
$$(5.10)$$

with $t_n = n\Delta t$, for $n = 1, \dots, N$ and $C_1, C_2 > 0$ are constants independent of h and Δt. Here $(c_h^n, s_h^n, \boldsymbol{u}_h^n, \boldsymbol{\omega}_h^n, p_h^n)$ denotes the sequence generated by (5.3) for all $n = 1, \dots, N$. A rigorous derivation of this space-time error estimate is part of ongoing developments.

6. **Numerical tests.** We finally present a set of elementary examples to illustrate the properties of the model and of the proposed finite element method. The coupling between Brinkman and reaction-diffusion equations will be implemented either via: a) a fully monolithic solution, b) an iterative Picard method splitting linear Brinkman and fully explicit reaction-diffusion equations, and c) an iterative Picard method with an embedded Newton algorithm for the linearisation of the reaction-diffusion system. Rigorous convergence proofs for the Newton iteration and various linear iterative schemes applied to similar problems in non-viscous flow in porous media can be found in e.g. [27, 34]. For our particular scenario, efficient coupling
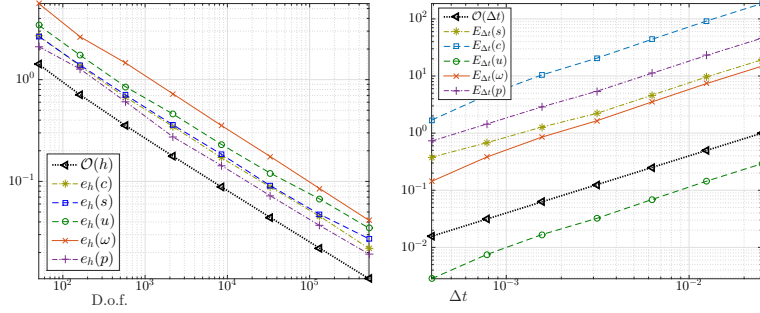
FIGURE 1. Example 1. Convergence tests for the spatial (left) and temporal (right) discretisation via mixed $\mathbb{P}_1 \times \mathbb{P}_1 \times \mathbb{RT}_0 \times \mathbb{P}_1 \times \mathbb{P}_0$ finite elements and backward Euler time stepping applied to (2.1).

strategies and thorough comparisons between dedicated solvers have been reported in [24].

Example 1. Spatio-temporal accuracy. Let us consider the spatio-temporal domain $\Omega_T = (0,1)^2 \times (0,0.1]$ and define the following exact solutions to (2.1) in the case of constant diffusivities D_c, D_s:

$$c(\boldsymbol{x},t) = \exp(-4D_c\pi^2 t)[\cos(2\pi x) + \cos(2\pi y)],$$

$$s(\boldsymbol{x},t) = \exp(-4D_s\pi^2 t)[\cos(2\pi x) + \cos(2\pi y)], \quad p(\boldsymbol{x},t) = x^4 - y^4,$$

$$\boldsymbol{u}(\boldsymbol{x},t) = 3\sin(t)x^2(x-1)^2y^2(y-1)^2\big(x(x-1)(2y-1), -(2x-1)y(y-1)\big)^T,$$

$$\boldsymbol{\omega}(\boldsymbol{x},t) = -6\sin(t)\sqrt{\mu}[x(5x^3 - 10x^2 + 6x - 1)y^3(y-1)^3$$
$$+ y(5y^3 - 10y^2 + 6y - 1)x^3(x-1)^3].$$

(6.1)

The model parameters are set as $\mu = 1$, $D_c = 0.01$, $D_s = 0.5$, $\boldsymbol{g} = (0,-1)^T$, and $\mathbb{K} = \mathbf{I}$; the reaction kinetics are specified by

$$G_j(c,s) = 6\pi\sin(t)\exp(-4D_j\pi^2 t)x^2(x-1)^2y^2(y-1)^2$$
$$\times [(2x-1)y(y-1)\sin(2\pi y) - x(x-1)(2y-1)\sin(2\pi x)], \quad j = c,s,$$

whereas $\boldsymbol{f}$ is computed using (6.1) and the momentum equation in (2.1). Note that these solutions satisfy the mass conservation equation, while boundary and initial conditions (2.2) are imposed according to (6.1). Also, a non-homogeneous source term is incorporated on the right hand side of the reaction-diffusion equations and constructed using the manufactured solutions.

DoF	163	579	2179	8451	33283	526339
avg(iter)	4.2	4.0	4.0	3.8	4.2	4.3

Example 1. Average number of Newton iterations to reach the residual tolerance tol$= 1e - 6$, according to the number of degrees of freedom in each refinement level.

Errors associated to splitting algorithms are avoided by invoking the exact full Jacobian and performing Newton iterations until convergence at each time step.

The mesh convergence is investigated by fixing Δt =1.6e-4 and computing errors between the exact solutions from (6.1) and approximations obtained with our mixed-primal method on a sequence of successively refined structured triangulations of Ω, at the final adimensional time T =5e-3. That is, for each field η, we compute $e_h(\eta) := \|\eta^N - \eta_h^N\|$, where $\eta^N = \eta(\cdot, T)$, and $\|\cdot\|$ is either the H^1, $H(\text{div})$, or L^2−norm. On the other hand, the error history associated to the time discretisation is studied by fixing a small meshsize $h = 2.43\text{e-}5$ and computing accumulative errors up to $T = 0.1$, and decreasing Δt. That is, we measure errors in the $\ell^\infty(0, t; \cdot)$−norm: $E_{\Delta t}(\eta) := \sum_{n=0}^{N} \|\eta^n - \eta_h^n\|_{(\cdot)}$. Figure 1 depicts a convergence analysis for the propose method with respect to meshsize and timestep. All plots indicate an overall first order convergence in both space and time, as expected from the involved approximations yielding (5.10). In Table 6 we provide the iteration count to reach convergence of the Newton method for the first test of spatial accuracy. The values represent the average of required steps at each resolution, and indicate that the convergence is independent of the refinement level.

Example 2. Bacterial bioconvection. Next we focus on the interaction between bacteria (with concentration c) and oxygen (described by s) in a small chamber, similar to the case studied in e.g. [23]. Let us define the function $r(s) = -\frac{\alpha}{2}(1 + \frac{s-s^*}{\sqrt{(s-s^*)^2+\varepsilon^2}})$, where s^* is an oxygen threshold, below which the chemotactic convection is turned off. We consider a semi implicit approximation of the cross diffusion, the reaction part for the oxygen conservation equation is given by $G_s(c, s) = \beta c r(s)$, and the remaining model functions and adimensional parameters are set as follows: $\mathbb{K} = K_0 + K_0 \eta(x)$ (with $K_0 = 7700$ and η a uniformly distributed random field), $g = (0, -\gamma)^T$, $s^* = 0.3$, $D_c = 0.01$, $D_s = 0.25$, $\varepsilon = h$. The computational domain is a disk of radius $\frac{1}{2}$ centred at $(\frac{1}{2}, \frac{1}{2})$, discretised into an unstructured mesh of 13972 points and 27942 triangular elements, and a timestep of Δt =1e-3 is employed. For this example we solve via fixed point iterations the coupling between the Brinkman problem and the set of reaction-diffusion equations. The system is initially at rest (zero velocity, vorticity, and pressure), having a concentration of bacteria near the top of the disk $c_0 = 1 - (1 + \exp(-50\sqrt{(x-0.5)^2 + (y-0.9)^2}))^{-1}$, and an homogeneous oxygen content $s_0 = 1$. In Figure 2 we show three snapshots (at advanced time) of the obtained numerical solutions on different regimes characterised by α, β, γ. In all cases we observe the species heading to the bottom of the disk, generating vortical flow around the zones of high concentrations of oxygen and bacteria. The plots indicate that transitional flow occurs (mainly due to the triggering of unstable modes), which can be captured in a robust manner by the numerical method, even in the most unstable regime.

Example 3. FitzHugh-Nagumo dynamics in a porous cavity. This test emphasises the effects of high contrast permeabilities on the propagation of travelling waves dictated by the well-known FitzHugh-Nagumo reactions $G_c(c, s) = k(s + c(c-a)(c-1))$, and $G_s(c, s) = d_1 c - s$. In this prototype model of excitable systems, c and s represent a membrane voltage, and a recovery variable. We consider a rectangular domain $\Omega = (0, 1.8) \times (0, 1)$ filled with 60 large particles (of radii 0.0015 and located randomly). The forcing terms are $\boldsymbol{g} = \sqrt{2}d_2(1, 1)^T$ and $\boldsymbol{f} = \boldsymbol{0}$. Moreover, the conductivity of the medium is assumed anisotropic and affected by the heterogeneity of the permeability field $(D_c)_{1,1} = 40\mathbb{K}$, $(D_c)_{2,2} = 5\mathbb{K}$, D_s =1e-3, the fluid viscosity is $\mu = 0.01$, and the remaining parameters are chosen as $a = 0.25$, $d_1 = 0.16875$, $d_2 = 250\sqrt{3}$, $k = -100$. The mesh has 28712 elements sharing 14581 nodes, we
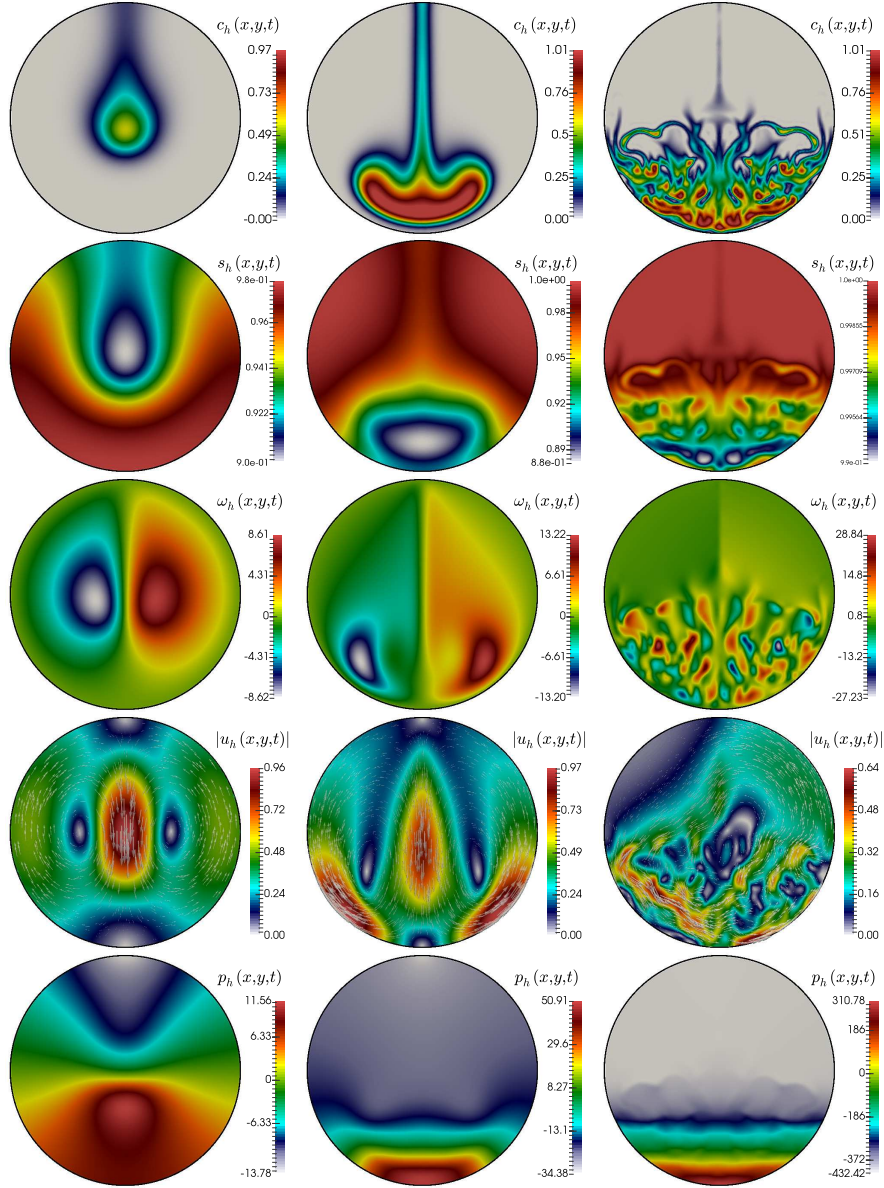
FIGURE 2. Example 2: snapshots at $t = 0.5$ of the bioconvection dynamics for three different regimes characterised by $\alpha = \beta = 0.1, \gamma = 41.8$ (left), $\alpha = 0.25, \beta = 2.5, \gamma = 418$ (centre), and $\alpha = \beta = 5, \gamma = 4180$ (right). Computed solutions from top to bottom: bacteria concentration, amount of oxygen, vorticity, velocity, and pressure.

set a timestep of $\Delta t = 2.5\text{e-}3$, and run the simulation until $T = 6$. First, we use the method of characteristics to treat the advective terms, whereas the reaction kinetics are considered explicit. The obtained numerical solutions are depicted in Figure 3. We investigate the convergence properties of the coupling schemes. In a
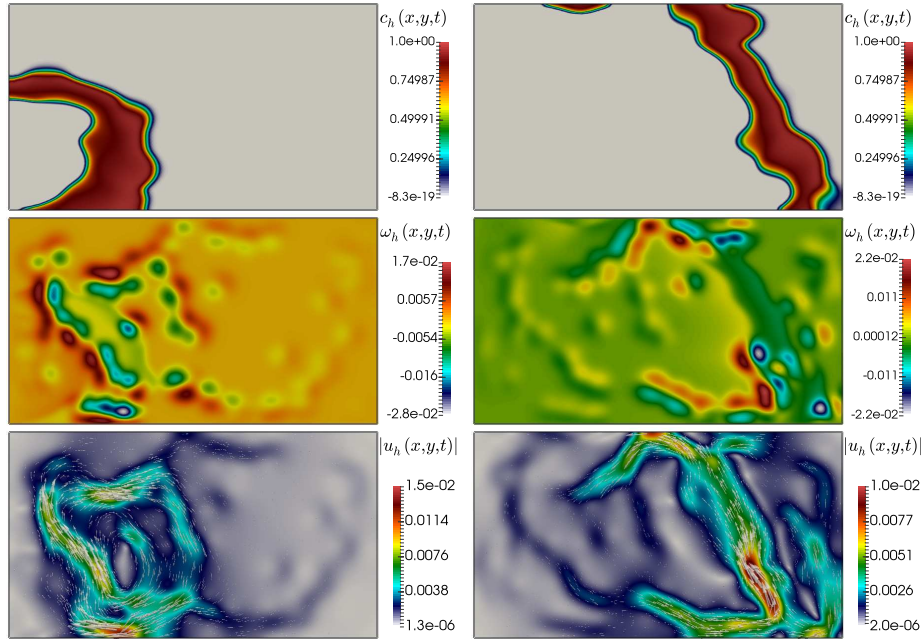
FIGURE 3. Example 3A: snapshots of FitzHugh-Nagumo dynamics on a porous mixture at early (left) and advanced (right) times. Computed solutions from top to bottom: membrane voltage, vorticity, and velocity.

second round of tests we now use a Picard iterative iterative scheme to couple the Brinkman and the FitzHugh-Nagumo equations, and consider the reaction terms implicitly, so that an embedded Newton iteration is applied inside each fixed-point solution. Figure 4 portrays the evolution of the number of required outer fixed-point and inner Newton steps to achieve convergence (set with a tolerance of tol=$1e-6$ for both schemes). We see that the number of Picard steps needed to converge are higher at the beginning of the simulation and they slowly decrease, whereas the Newton steps applied to the nonlinear reaction terms do not change substantially.

We also perform the 3D counterpart of this example, defined in the polygonal domain $\Omega = (0, 1.8) \times (0, 1) \times (0, 0.6)$ filled with 60 large particles (of radii 1.5e-3 and randomly distributed on Ω) with a permeability 100 times higher than in the rest of the porous matrix. The forcing term is specified by $\boldsymbol{g} = d_2(1, 1, 1)^T$ and $\boldsymbol{f} = \boldsymbol{0}$, whereas the conductivity matrix and remaining parameters are chosen as above. The domain is discretised into an unstructured mesh of 126034 tetrahedral elements sharing 21952 nodes, and the same timestep as above is employed. All sides of the box are provided with zero-fluxes for voltage and recovery fields, zero tangential vorticity, and zero normal velocities, and as initial condition we excite the bottom left part of the domain. For this test a Newton algorithm is used to linearise the reaction-diffusion equations, and outer Picard iterations are applied to couple that system together with the set of Brinkman equations. The obtained numerical solutions are depicted in Figure 6. As in its 2D counterpart, in this test we notice that a propagating front for the potential moves towards the positive x−axis, followed by the slower recovery variable front. Due to the heterogeneity of
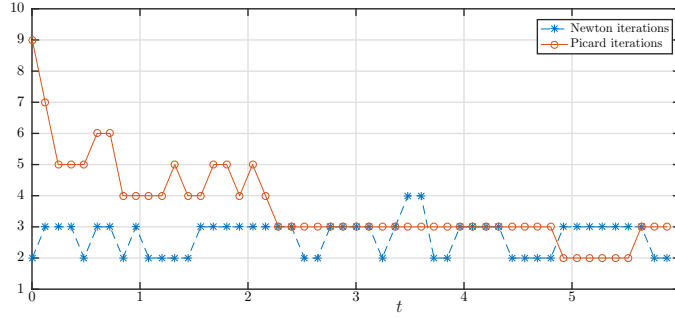
FIGURE 4. Example 3A: Number of inner Newton steps and outer Picard steps needed to reach residual convergence to a tolerance of 1e-6.
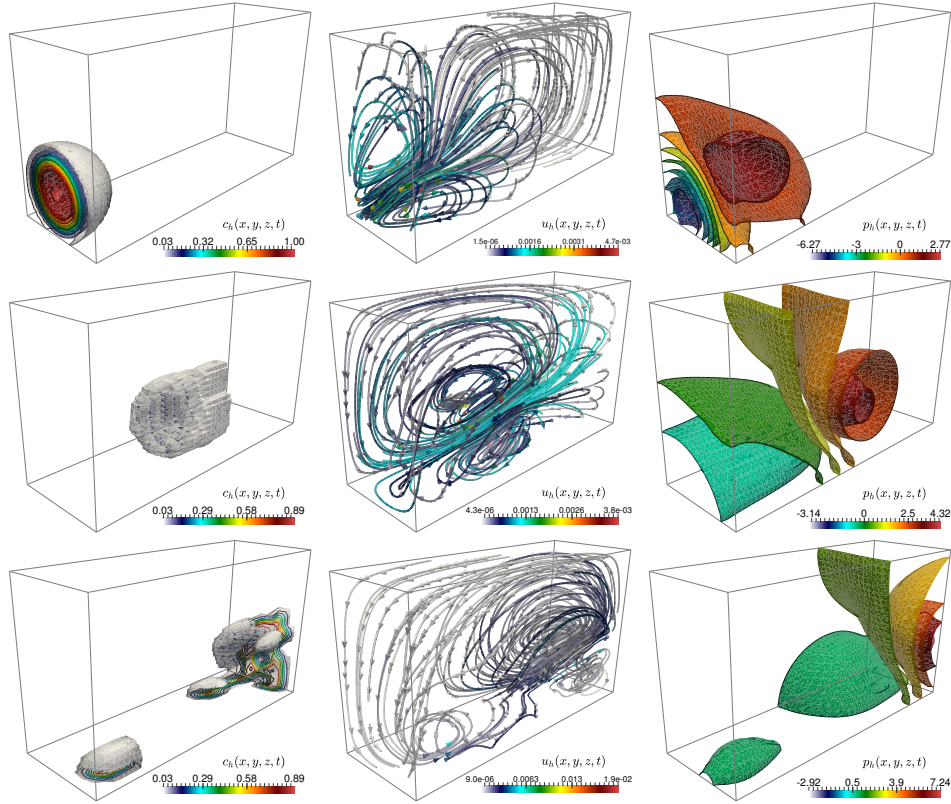
Example 3B. Approximate membrane voltage, velocity, and pressure for the FitzHugh-Nagumo dynamics on a porous mixture at early (top), moderate (middle row), and advanced (bottom panels) times.

conductivities and permeabilities, preferential velocity patterns start to form. We also notice that vorticity (in this case, we show only its magnitude) clearly marks the regions of contact between high gradients of potential and recovery field.
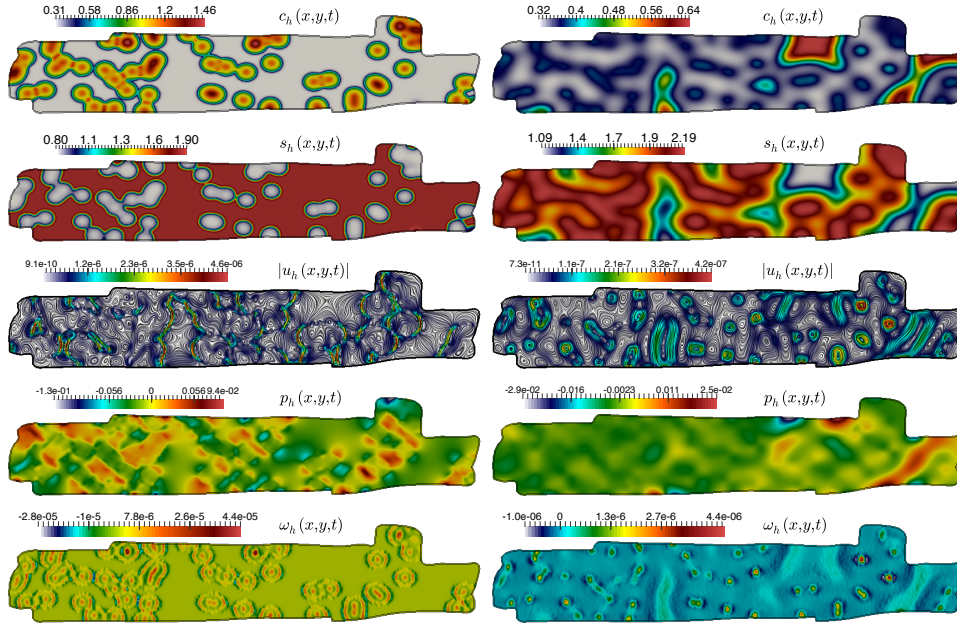
FIGURE 5. Example 4: Computed solutions (cytosolic calcium, sarcoplasmic calcium, vorticity, velocity, and pressure) for the intracellular calcium dynamics at early (left) and advanced (right) times.

Example 4. Intracellular calcium-induced calcium release. In closing this section we present a simulation of the interaction between two species c, s (the concentrations of cytosolic and sarcoplasmic calcium, respectively) inside a cardiac cell. This phenomenon has been studied in terms of the reacting species alone (*cf.* [18, 26]), and also including the active cell contraction while solving for the underlying finite elasticity equations [29, 38]. In contrast, here we assume that the species interact with an interstitial fluid occupying the sarcoplasmic reticulum, which is in turn pictured as a porous medium with a non-homogeneous permeability distribution. A 2D geometry reconstructed from confocal images is used and a triangular mesh of 46610 elements and 23741 vertices is generated. The time advancing algorithm uses a fixed time step of $\Delta t = 0.01$. The process consists in opening 80 channels of cytosolic calcium located randomly within the myocyte, and observing how these propagate thorough plasma into the whole cell. We also consider that the permeability is higher in the vicinity of these channels. The minimal reaction-diffusion model proposed in [18] involves the following specialisation for constant and species-dependent coefficients:

$$D_c = (1 + \frac{1}{4}\eta(\boldsymbol{x})) \begin{pmatrix} 0.6 & 0 \\ 0 & 0.3 \end{pmatrix}, \ D_s = 0.01,$$

$$G_c(c, s) = \nu_1 - \nu_2 \frac{c^2}{k_2 + c^2} + \nu_3 \frac{c^4 s^2}{(k_3 + s^2)(k_4 + c^4)} - \nu_4 c,$$

$$G_s(c, s) = \nu_2 \frac{c^2}{k_2 + c^2} - \nu_3 \frac{c^4 s^2}{(k_3 + s^2)(k_4 + c^4)} - \nu_5 s,$$

where η is a step function assuming the value 1 on disks centred at uniformly distributed random locations corresponding to the channels, and zero elsewhere. The influence of calcium patterns into the flow behaviour of the plasma is encoded in the forcing term for the momentum equation $\boldsymbol{f}(s) = \gamma_0 |s| (\boldsymbol{f}_0 \otimes \boldsymbol{f}_0) \nabla s$, which might be regarded as the flow-counterpart to the active force proposed in [28]. Here $\boldsymbol{f}_0 = (1,0)^T$ is a given preferential direction of plasma displacement, and the remaining parameters are $\gamma_0 = -0.12$, $\nu_1 = 1.58$, $\nu_2 = 16$, $\nu_3 = 91$, $\nu_4 = 2$, $\nu_5 = 0.2$, $k_2 = 1$, $k_3 = 4$, $k_4 = 0.75$, $\mathbb{K} = 1\text{e-4}(1 + 10\eta(\boldsymbol{x}))$. Snapshots of the numerical solutions at an early and advanced time steps are collected in Figure 5. Starting from the open channels, the cytosolic calcium starts to propagate towards other channels, also following a higher diffusion in the preferential direction $\boldsymbol{f}_0$ (aligned with the $x-$axis).

7. **Concluding remarks.** The interaction of viscous flow in porous media and reaction-diffusion phenomena occur in a variety of applicative scenarios. Here we have advocated the solvability analysis and the numerical approximation of a special class of problems related to Brinkman and nonlinear advection-diffusion-reaction equations. The analysis of the coupled set of equations is framed under the theory of fixed-point schemes combined with an abstract result for saddle-point problems. A mixed-primal finite element method has been proposed and we have discussed its stability and convergence properties. We have provided numerical validation of the spatio-temporal convergence of the method, and have also addressed the simulation of a number of biochemically-oriented examples.

Our theoretical framework currently does not account for higher order terms nor the chemotactical convection simulated in Example 2, and further investigation is needed in this direction. We also need to cover the dependence of the momentum force on the gradient of the chemical concentrations (studied numerically in Example 4). Regarding other model generalisations, interesting topics be explored include cross-diffusion effects, nonlinear convective fluxes, a non-laminar flow regime, viscosity depending on the chemical concentrations, or variable density flows. Finally, we mention that the study of mixed formulations involving embedded saddle-point problems and the convergence analysis of the associated fully-mixed finite element schemes can be the subject of suitable extensions to the mathematical aspects of this contribution.

REFERENCES

[1] A. Agosti, L. Formaggia and A. Scotti, Analysis of a model for precipitation and dissolution coupled with a Darcy flux, *J. Math. Anal. Appl.*, **431** (2015), 752–781.

[2] A. Agouzal and K. Allali, Numerical analysis of reaction front propagation model under Boussinesq approximation, *Math. Meth. Appl. Sci.*, **26** (2003), 1529–1572.

[3] V. Anaya, G. N. Gatica, D. Mora and R. Ruiz-Baier, An augmented velocity-vorticity-pressure formulation for the Brinkman equations, *Int. J. Numer. Methods Fluids*, **79** (2015), 109–137.

[4] V. Anaya, D. Mora, R. Oyarzúa and R. Ruiz-Baier, A priori and a posteriori error analysis of a fully-mixed scheme for the Brinkman problem, *Numer. Math.*, **133** (2016), 781–817.

[5] V. Anaya, D. Mora, C. Reales and R. Ruiz-Baier, Stabilized mixed approximation of axisymmetric Brinkman flows, *ESAIM: Math. Model. Numer. Anal.*, **49** (2015), 855–874.

[6] V. Anaya, D. Mora and R. Ruiz-Baier, Pure vorticity formulation and Galerkin discretization for the Brinkman equations, *IMA J. Numer. Anal.,* **37** (2017), 2020–2041.

[7] J.-L. Auriault, On the domain of validity of Brinkman's equation, *Transp. Porous Med.*, **79** (2009), 215–223.

[8] J. W. Barret and P. Knabner, Finite element approximation of the transport of reactive solutes in porous media. Part II: error estimates for equilibrium adsorption processes, *SIAM J. Numer. Anal.*, **34** (1997), 455–479.

[9] P. Biscari, S. Minisini, D. Pierotti, G. Verzini and P. Zunino, Controlled release with finite dissolution rate, *SIAM J. Appl. Math.*, **71** (2011), 731–752.

[10] H. Brezis, *Analyse Fonctionnelle. Théorie et Applications*, Masson, Paris, 1983.

[11] G. Chamoun, M. Saad and R. Talhouk, A coupled anisotropic chemotaxis-fluid model: The case of two-sidedly degenerate diffusion, *Comput. Math. Appl.*, **68** (2014), 1052–1070.

[12] C. M. Elliott and B. Stinner, A surface phase field model for two-phase biological membranes, *SIAM J. Appl. Math.*, **70** (2010), 2904–2928.

[13] A. Ern and V. Giovangigli, *Multicomponent Transport Algorithms*, vol. 24 of Lecture Notes in Physics, New Series Monographs, Springer-Verlag, Heidelberg, 1994.

[14] A. Ern, J. L. Guermond and L. Quartapelle, Vorticity-velocity formulations of the Stokes problem in 3D, *Math. Methods Appl. Sci.*, **22** (1999), 531–546.

[15] L. Formaggia, S. Minisini and P. Zunino, Modelling polymeric controlled drug release and transport phenomena in the arterial tissue, *Math. Models Methods Appl. Sci.*, **20** (2010), 1759–1786.

[16] A. C. Fowler, Convective diffusion on an enzyme reaction, *SIAM J. Appl. Math.*, **33** (1977), 289–297.

[17] G. N. Gatica, *A Simple Introduction to the Mixed Finite Element Method. Theory and Applications*, Springer Briefs in Mathematics, Springer, Cham Heidelberg New York Dordrecht London, 2014.

[18] A. Goldbeter, G. Dupont and M. J. Berridge, Minimal model for signal-induced Ca^{2+} oscillations and for their frequency encoding through protein phosphorylation, *Proc. Natl. Acad. Sci. USA,* **87** (1990), 1461–1465.

[19] Q. Hong and J. Krauss, Uniformly stable discontinuous Galerkin discretization and robust iterative solution methods for the Brinkman problem, *SIAM J. Numer. Anal.*, **54** (2016), 2750–2774.

[20] K. Kumar, I. S. Pop and F. A. Radu, Convergence analysis for a conformal discretization of a model for precipitation and dissolution in porous media, *Numer. Math.*, **127** (2014), 715–749.

[21] T. Kuusi, L. Monsaingeon and J. Videman, Systems of partial differential equations in porous medium, *Nonl. Anal.*, **133** (2016), 79–101.

[22] O. A. Ladyženskaja, V. A. Solonnikov and N. N. Ural'ceva, *Linear and Quasi-linear Equations of Parabolic Type*, American Mathematical Society, 1988.

[23] H. G. Lee and J. Kim, Numerical investigation of falling bacterial plumes caused by bioconvection in a three-dimensional chamber, *Eur. J. Mech. B/Fluids*, **52** (2015), 120–130.

[24] P. Lenarda, M. Paggi and R. Ruiz Baier, Partitioned coupling of advection-diffusion-reaction systems and Brinkman flows, *J. Comput. Phys.*, **344** (2017), 281–302.

[25] H. Murakawa, Error estimates for discrete-time approximations of nonlinear cross-diffusion systems, *SIAM J. Numer. Anal.*, **52** (2014), 955–974.

[26] C. Nagaiah, S. Rüdiger, G. Warnecke and M. Falcke, Adaptive numerical simulation of intracellular calcium dynamics using domain decomposition methods, *Appl. Numer. Math.*, **58** (2008), 1658–1674.

[27] F. A. Radu and I. S. Pop, Newton method for reactive solute transport with equilibrium sorption in porous media, *J. Comput. and Appl. Math.*, **234** (2010), 2118–2127.

[28] R. Ruiz-Baier, Primal-mixed formulations for reaction-diffusion systems on deforming domains, *J. Comput. Phys.*, **299** (2015), 320–338.

[29] R. Ruiz-Baier, A. Gizzi, S. Rossi, C. Cherubini, A. Laadhari, S. Filippi and A. Quarteroni, Mathematical modeling of active contraction in isolated cardiomyocytes, *Math. Medicine Biol.*, **31** (2014), 259–283.

[30] R. Ruiz-Baier and I. Lunati, Mixed finite element – discontinuous finite volume element discretization of a general class of multicontinuum models, *J. Comput. Phys.*, **322** (2016), 666–688.

[31] B. Saad and M. Saad, A combined finite volume-nonconforming finite element scheme for compressible two phase flow in porous media, *Numer. Math.*, **129** (2015), 691–722.

[32] J. N. Shadid, R. S. Tuminaro and H. F. Walker, An inexact Newton method for fully coupled solution of the Navier-Stokes equations with heat and mass transport, *J. Comput. Phys.*, **137** (1997), 155–185.

[33] J. Simon, Compact sets in the space $L^p(0, T; B)$, *Ann. Mat. Pura Appl. (4)*, **146** (1987), 65–96.

[34] M. Slodicka, A robust and efficient linearization scheme for doubly nonlinear and degenerate parabolic problems arising in flow in porous media, *SIAM J. Sci. Comput.*, **23** (2002), 1593–1614.

[35] G. Tauriello and P. Koumoutsakos, Coupling remeshed particle and phase field methods for the simulation of reaction-diffusion on the surface and the interior of deforming geometries, *SIAM J. Sci. Comput.*, **35** (2013), B1285–B1303.

[36] R. Temam, *Navier-Stokes Equations. Theory and Numerical Analysis*, Reedition in the AMS-Chelsea Series, AMS, Providence, 2001.

[37] V. Thomée, *Galerkin Finite Element Methods for Parabolic Problems*, 2nd edition, Springer-Verlag, Berlin Heidelberg, 2006.

[38] P. Tracqui and J. Ohayon, An integrated formulation of anisotropic force-calcium relations driving spatio-temporal contractions of cardiac myocytes, *Phil. Trans. Royal Soc. London A*, **367** (2009), 4887–4905.

E-mail address: vanaya@ubiobio.cl
E-mail address: mostafa.bendahmane@u-bordeaux.fr
E-mail address: dmora@ubiobio.cl
E-mail address: ruizbaier@maths.ox.ac.uk